TÉCNICO LISBOA

# Solution Preparation in Pharmaceutical Processes: Dynamics and Dissolution models

**Tiago Alexandre Duarte Faustino**

Thesis to obtain the Master of Science Degree in

## Chemical Engeneering

Supervisors: Prof. Carla Isabel Costa Pinheiro
Eng Tiago Porfirio Fonseca - Hovione Farmaciencia S.A.

### Examination Committee

Chairperson: Prof. Maria Cristina De Carvalho Silva Fernandes

Members of the Committee: Eng. Tiago Porfirio Fonseca- Hovione Farmaciencia S.A.
Prof. João Pedro Martins de Almeida Lopes

**December 2021**

This page was intentionally left blank.

# Acknowledgments

I would first like to thank my supervisors, Professor Carla Isabel Costa Pinheiro and Engineer Tiago Porfirio Fonseca, for not only their invaluable expertise and insight into formulating the research questions and methodology but sharing their knowledge and supporting me whenever necessary to their fullest extent in order to make this thesis possible. Their, insightful feedback has pushed me to sharpen my thinking and brought my work to a higher level.

I would like to acknowledge Hovione Farmaciencia S.A as well as all the people involved during my internship for their wonderful collaboration and support as well as for all of the opportunities I was given to further my research and develop myself as a person.

In addition, I would like to thank my parents for their wise counsel and sympathetic ear. Finally, I could not have completed this dissertation without the support of my friends and colleagues who provided stimulating discussions as well as happy distractions to rest my mind outside of my research.

To each and every one of you – Thank you.

# Abstract

The dissolution of powders in liquids is a state of the art procedure essential to support pharmaceutical processes such as chemical and biological reactions, crystallization, coating and spray drying operations. Nevertheless, the intention behind the applicability of pharmaceutical grade powder dissolution lies in the desire to obtain a clear solution in the absence of solids in the most clean and efficient way. Traditionally, this step is performed in batch mode which depending of the material´s properties and the scale of the operation can take several hours or even days to be concluded affecting the efficiency and profitability of any operation. Thus, the feasibility, dynamics and applicability of dissolution models for a semi-continuous solution preparation process were studied to address all the shortcomings of traditional batch processing. Several dissolution tests were performed with different polymer-solvent pairs to establish a proof of concept while falling back on the aid of Process analytical technology (PAT) (viscometer, turbidimeter and refractive index (RI)) to asses some of the critical quality attributes (CQAs) and critical process parameter (CPPs) of the system. A total of 13 trials were performed, all presenting a smooth dissolution with a dissolution time under 10 minutes with all trials reaching the target concentration. Additionally, residence time distributions (RTDs) were established via the outlet concentration of the polymer powder that was acting as a tracer under specific conditions. Overall most polymer-solvent pairs were found to be able to serve as a tracer under specific flowing regimes and conditions. RTD modelling using ideal reactor also showed that viscosity is linked to the model itself. Lastly, some polymer dissolution models based on the complex diffusion of solvent penetration and chain disengagement mechanics from the particle to the bulk of the solution were capable of mimicking the experimental results.

# Keywords

Continuous manufacturing, Polymer dissolution, Residence Time Distribution,Process analytical technology (PAT), Real-time process monitoring,

# Resumo

A dissolução de pós em líquidos é um procedimento de ponta essencial para apoiar processos farmacêuticos tais como reações químicas e biológicas, cristalização, operações de revestimento e secagem por atomização. No entanto, a intenção da aplicabilidade da dissolução do pó de qualidade farmacêutica reside no desejo de obter uma solução clara na ausência de sólidos da forma mais limpa e eficiente possível. Tradicionalmente, esta etapa é executada em modo batch o que, dependendo das propriedades do material e da escala da operação, pode levar várias horas ou mesmo dias para ser concluída, afetando a eficiência e rentabilidade de qualquer processo. Deste modo foram estudados, a viabilidade, dinâmica e aplicabilidade de modelos de dissolução para um processo de preparação de soluções em semi-contínuo com o objetivo de minimizar as deficiências do processamento por batch. Foram realizados vários testes de dissolução com diferentes pares de polímero-solvente para estabelecer uma prova de conceito, recorrendo-se a tecnologias analíticas de processo (PAT) (viscosímetro, turbidímetro e índice de refracção (RI)) para avaliar alguns dos atributos de qualidade críticos (CQAs) e parâmetros de processo críticos (CPPs) do sistema. No total, foram realizados 13 ensaios, todos apresentando uma dissolução suave com um tempo de dissolução inferior a 10 minutos, atingindo ainda a concentração alvo. Adicionalmente, foram estabelecidas distribuições de tempo de residência (RTDs) através da concentração de saída do pó de polímero que acuta como traçador. Em geral, verificou-se que a maioria dos pares de polímero-solvente era capaz de servir como marcador sob regimes e condições de fluxo específicos. A modelização de RTDs utilizando reatores ideais mostrou que a viscosidade está ligada ao próprio modelo. Finalmente, alguns modelos de dissolução de polímeros baseados na penetração do solvente por difusão e na mecânica de desengate da cadeia desde a partícula até ao grosso da solução foram capazes de representar os resultados experimentais.

# Palavras Chave

Produção continua, Dissolução polimérica; Distribuição de tempos de residência,Tecnologias analíticas de processo (PAT), Monitorização de processos em tempo real.

# Contents


**1 Introduction** **1**

1.1 Industry Background: Batch vs Continuous manufacturing . . . 2

1.2 Motivation . . . 3

1.3 Goals . . . 3

1.4 Dissertation Outline . . . 4

**2 Literature Review** **5**

2.1 Continuous/Semi-Continuous Manufacturing . . . 6

2.2 Polymers in the pharmaceutical Industry . . . 7

2.2.1 Polymer Solutions . . . 9

2.2.2 Polymer Rheology . . . 12

2.3 Material Tracking: Residence Time Distribution . . . 15

2.4 Process Monitoring . . . 20

2.4.1 PAT tools . . . 20

2.4.2 First Principles Dissolution Models . . . 23

2.4.3 Sensor Fusion and Soft sensors . . . 25

**3 Materials and Methods** **27**

3.1 Materials . . . 28

3.2 Methods . . . 30

**4 Process Dynamics and Modeling** **31**

4.1 Process Dynamics: Residence Time Distributions . . . 32

4.1.1 Methodology . . . 32

4.1.2 Consistency Tests . . . 34

4.1.3 Real Reactor Modeling based on Ideal reactors . . . 36

4.2 Polymer dissolution Models . . . 38

4.2.1 Vrentas and Vrentas (1998) Model . . . 38

4.2.2 Devota *et al* (2014) Model . . . 39

4.2.3 Parameter Estimation and Evaluation . . . 40

**5 Results and Discussion** **43**
5.1 Experimental: PAT results and observations . . . 44
5.2 Residence Time distributions . . . 44
5.2.1 Reynolds Assessment . . . 45
5.2.2 Experimental RTD and Mean residence time . . . 49
5.2.3 Consistency Tests . . . 54
5.2.4 RTD modeling based on ideal reactors . . . 56
5.3 Modeling of Polymer dissolution . . . 60
**6 Conclusions and Future Work** **63**
6.1 Conclusions . . . 64
6.2 Future Work . . . 65
**Bibliography** **67**
**A Appendix** **73**
A.1 Polymers and Nomenclature . . . 73
A.2 Methodology-Dissolution Tests . . . 73
A.3 Experimental Dissolution Results . . . 74

# List of Figures


2.1 Representation of two-dimensional Flory-Huggins lattice [1]:(a) Model for a low molecular weight solute in a solvent; (b) Model for a polymer chain in solution . . . . . 10
2.2 A schematic of one-dimensional solvent diffusion and polymer dissolution. (Adapted from Ref [2] . . . . . 10
2.3 Schematic picture of the composition of the surface layer. (Adapted from Ref [3] . . . . . 11
2.4 Newtonian Flow: Couette Flow with no pressure gradient . . . . . 13
2.5 Polymer Rheology:Shear-Thinning behaviour . . . . . 14
2.6 Refraction Index Background:Refraction of a Light ray . . . . . 20
2.7 First principle polymer Dissolution models and their constraints and assumptions . . . . 24

3.1 Summary of the polymers used and their properties/applications . . . . . 29
3.2 Hydramotion vibrational viscometer . . . . . 30

4.1 Schematic representation of the conditions required for Polymers to be used as tracer in the existing systems. Adapted from [4] . . . . . 34
4.2 Association of Reactor in series with know RTDs . . . . . 37

5.1 Reynolds assessment over the solids dissolution time for $P_1$ systems, trials #1; #2,#3; #5; #7 and #8: (a) Reynolds assessment for $P_1$ in 80:20 %w/w of DCM and Methanol (b) Reynolds assessment for $P_1$ in Methanol (c) Reynolds assessment for $P_1$ in Acetone . . . 47
5.2 Reynolds assessment over the solids dissolution time for $P_2$ systems, trial #9; #10 and #11: (a) Reynolds assessment for $P_2$ in 80:20 %w/w of DCM and Methanol (b) Reynolds assessment for $P_2$ in Methanol . . . . . 48
5.3 Reynolds assessment over the solids dissolution time for $P_3$ systems, trial #12; and #13 . 49
5.4 Experimental Residence Time distributions for each system determination by step administration of tracer: (a)Trial #1 (b) Trial #2 (c) Trial #3 . . . . . 50
5.5 Experimental Residence Time distributions for each system determination by step administration of tracer: (a)Trial #5 (b) Trial #7 . . . . . 52

5.6 Experimental Residence Time distributions for each system determination by step administration of tracer: Trial #8 . . . 52
5.7 Experimental Residence Time distributions for each system; determination by step administration of tracer: Trial #9 . . . 53
5.8 Experimental Residence Time distributions for each system determination by step administration of tracer: (a)Trial #12 (b) Trial #13 . . . 54
5.9 Trial #5 Modeling Response . . . 57
5.10 Trial #5 Concentration Prediction vs Experimental . . . 57
5.11 Trial#7 Modeling Response . . . 57
5.12 Trial #7 Concentration Prediction vs Experimental . . . 57
5.13 Modeling of the experimental residence time distributions for trial #8 and its corresponding concentration prediction . . . 58
5.14 Experimental Residence Time distributions for each system determination by step administration of tracer: (a)Trial #5 (b) Trial #7 . . . 59
5.15 Trial #12 Modeling response . . . 59
5.16 Trial #12 Concentration prediction vs experimental . . . 59
5.17 Trial#13 Modeling response . . . 59
5.18 Trial #13 Concentration Prediction vs Experimental . . . 59
5.19 Polymer dissolution model concentration profiles and its comparison to the experimental data: (a)-Trial #8-$P_1$ in Acetone at 8% w/w (b)-Trial #12 $P_3$ in Acetone at 8%w/w (c)-Trial #13 $P_3$ in Acetone at 10% w/w . . . 60

# List of Tables


1.1 Batch vs Continuous Manufacturing [5] [6] . . . . . 2

5.1 Overview of the result Dissolution trials/PoC for each Polymer:Solvent system - Average dissolution times . . . . . 44

5.2 Overview of the trials analyses for experimental determination of RTDs . . . . . 45

5.3 Upper and Lower limits for the Reynolds number of each trial.** Trial marked red are trials whose variation far exceed the upper and lower limits throughout this evaluation . 46

5.4 Mean residence times for $P_1$ in DCM:MeOH(80:20) systems for different trials under different conditions. Trial #1 $T_0 = 19,5^{\circ C}$ and 5125 rpm during solids incorporation. Trials #2 and #3 $T_0 = 5.2^{\circ C}$ and $4.5^{\circ C}$ respectively . . . . . 49

5.5 Mean residence times for $P_1$ in MeOH under different recirculating flowrates, Trial #5 5125 rpm and Trial #7 7295 rpm . . . . . 51

5.6 Mean residence time for $P_1$ in Acetone systems- trial #8 . . . . . 52

5.7 Mean residence time for $P_2$ in DCM:MeOH(80:20) systems- trial #9 . . . . . 53

5.8 Mean residence times for $P_3$ in Acetone under different conditions. Trial #12-$C_{tracer} = 8\%w/w$. Trials #13- $C_{tracer} = 10\%w/w$ . . . . . 53

5.9 Comparison between the inlet and outlet tracer amount for the consistency tests . . . . . 55

5.10 Quantification of the bypass and dead volume when compared to existing flow rate and rector volume . . . . . 56

5.11 Vrentas and Vrentas Rubbery dissolution model parameters.** Values obtained from literature [7] [8] . . . . . 61

5.12 Vrentas and Vrentas Glassy dissolution model parameters.** Values obtained from literature [7] [8] . . . . . 62

5.13 Devota *et al.* (2014) dissolution model parameters.** Values obtained from literature [7] [8]. 62

# Acronyms

**APIs** (Active Pharmaceutical Ingredients)

**ASDs** (Amorphous solid dispersions)

**CM** (Continuous manufacturing)

**CPP** (Critical process parameters)

**CQA** (Critical Quality attributes)

**FDA** (Food and Drug administration)

**FTU** (Active Pharmaceutical Ingredients)

**LF** (Laminar Flow model)

**MT** (Material Tracking)

**NTU** (Nephelometric Turbidity unit)

**NIR** (Near infra-red spectroscopy)

**PAT** (Process Analytical Technology)

**PD** (Polymer Dissolution)

**PFR** (Plug Flow Reactor)

**PoC** (Proof of Concept)

**QbD** (Quality by design)

**RI** (Refractive Index)

**RTD** (Residence Time distribution)

**RTRT** (Real Time Release Testing)

# 1

# Introduction

## Contents


1.1 Industry Background: Batch vs Continuous manufacturing . . . . . 2

1.2 Motivation . . . . . 3

1.3 Goals . . . . . 3

1.4 Dissertation Outline . . . . . 4

## 1.1 Industry Background: Batch vs Continuous manufacturing

As we enter into a new decade, corporations have long sought better approaches to material processing. Nevertheless, at the cornerstone of any development and despite all the effort, lies the never-ending debate of which type of process can provide better long term results: batch processing or continuous flow.

Batch processes are usually defined as a sequence of one or more steps that should be performed in a pre-arranged order. Nevertheless, this strategy has a myriad of drawbacks, that range from its high processing time, to quality discrepancies between each batch [9], [5] [6]; as well as often falling back on the user´s experience and knowledge to control and assess most critical quality attributes (CQAs) despite the extensive guidelines and requirements of regulators to reduce uses visual checks as a control strategy when implementing new processes.

On the other hand, a continuous or semi-continuous process involves product manufacturing without any breaks in, substance, sequence or extent at every step of the process. As the name suggests, the flow of product or material is continuous and every machine operates in a steady state and has a certain processing function. Thus, the major drawback of this processing method is the increasing risk of contaminating materials. However, with proper design and technology, continuous or semi-continuous processing can offer much faster operations, better quality, and scalability, while simultaneously adapting to the needs of the industry more efficiently than batch processing operations [5] [6].

As such, having a deeper understanding of the industry and the general advantages and disadvantages of each processing method can improve the profitability of any project as well as provide better foundations for future improvements. Therefore,in table 1.1 lies a general summary of the key pluses and minuses to each mode of operation.

**Table 1.1:** Batch vs Continuous Manufacturing [5] [6]

| Parameter | Batch | Continuous |
|---|---|---|
| **Coordination** | Step by Step approach | Machines have specific functions and operate at steady state |
| **Quantities Produced** | A unit is produced | Large Quantities |
| **Fouling** | High fouling expectations | Low fouling expectations |
| **Equipment costs** | Low cost | High cost |
| **Control options** | Easy control strategies | More sophisticated control strategies |
| **Shut down Times** | Often | Rare |
| **Manpower** | Lack of automation makes necessary a larger workforce | Can be fully automated |

In the Pharmaceutical Industry, on the other hand, due to the fact that most medicine

in the market is consumed either orally or via inhalers through micro-particles in solid dosage forms, more advanced therapeutic approaches have created complex requirements that impact conventional processing techniques such as spray drying, hot melt extrusion, wet chemistry, crystallization and phase separation processes, [9] [2] creating additional strain and stress in the upstream operations such as solution preparation that carries a paramount importance in the overall manufacturing operation. That said, contrary to the conventional batch approach, where a reactor is manually charged with a solvent mixture and other ingredients such as APIs (Active pharmaceutical ingredients) and polymers powders (usually excipients), the implementation of a continuous or semi-continuous strategy can not only increase productivity but also reduce operating costs and ensure a higher degree of product quality. Some examples of these shift are in the production of amorphous solid dispersions (ASDs), or when using coating agents or surfactants in micro-encapsulation or lipid formulation. [10] [11].

## 1.2 Motivation

The motivation behind this work lies in understanding and gaining further insight into how a semi-continuous solution preparation strategy can answer some fundamental problems regarding the conventional batch approach such as the proper dispersion of the powder mixes and the determination of the dissolution end points, since they are typically confirmed visually by a technician/operator. Furthermore, another motivation of this work lies in the understanding of the thermodynamics of some of the most used drug-polymer systems in the pharmaceutical industry in order to lay the ground work for the development of material tracking and process monitoring and control strategies, in an attempt to establish a stable process capable of being scaled up and implemented in the future. Additionally, the formation of gums and aggregates in the reactor walls, stirrers and probes that are typical in polymer dissolution in the pharmaceutical industry were also taken into account.

## 1.3 Goals

In light of the above the current work is aimed to assess the process dynamics of a pilot scale unit for the semi-continuous preparation of solutions used in typical drug formulations that can be implemented in any industrial process for the production of solid dispersions. Therefore as a result it is also necessary to lay the groundwork to create

material tracking and process control strategies in an attempt to establish a stable process capable of being scaled up and implemented in the future:

To accomplish this, we have the following sub-goals:

1. Establish a manual proof of concept (PoC) of an existing process at pilot-level scale, by determining dissolution end points and concentration profiles of specific polymer/solvent pairings, while, simultaneously assessing and understanding the role and impact of certain critical quality attributes (CQAs) of the product with process conditions.

2. Assess residence time distributions of the existing set-up with the goal of characterizing the operating unit for future automatic control options

3. Assess the possibility of using semi-empirical polymer dissolution models to reproduce the experimental data and combine both model and experimental results in order to create hybrid sensor fusion strategies that can prevent some of the known limitations of the process analytical technology (PAT) that were used, such as sensor saturation and the inability of predicting future behavior

## 1.4 Dissertation Outline

Chapter 2 presents a review on the existing literature of preparing polymer solutions, more specifically the interactions between polymers and solvents during the dissolution process as well as the current techniques used to establish residence time distributions and process monitoring strategies, PAT and semi-empirical models (2: Literature Review). Chapter 3 is dedicated to the the materials and methods that were used throughout the work in order to establish the PoC and assess the dynamics of the process (3: Raw Materials and Methods). Chapter4 presents a more in depth analysis of the process dynamics and modeling strategies that were utilized (4: Process Dynamics and Modeling). Afterwards, Chapter 5 is dedicated to all the experimental and modeling results that were obtained throughout this work as well as an in-depth explanation and analysis of such results (5: Results and Discussion) and lastly chapter 6 presents the conclusions of the overall work as well as some of the future application and suggestions for future work

# 2

# Literature Review

## Contents


2.1 Continuous/Semi-Continuous Manufacturing . . . . . 6

2.2 Polymers in the pharmaceutical Industry . . . . . 7

2.3 Material Tracking: Residence Time Distribution . . . . . 15

2.4 Process Monitoring . . . . . 20

## 2.1 Continuous/Semi-Continuous Manufacturing

In FDA´s "Process Validation: General Principles, 2010" [12] [13], pharmaceutical regulators express the idea that continuous manufacturing (CM) or semi-continuous manufacturing (SCM) can improve pharmaceutical manufacturing by using integrated processes with fewer steps and shorter processing times, while also achieving smaller equipment footprints and supporting an enhanced development approach (e.g. Quality by Design (QbD) and the usage of PAT tools and models). Therefore, in a transition between batch and t continuous operations the introduction of continuous elements in the process is expected to enable real time product quality monitoring and provide an easier scale-up options for all manufacturers [13]. Traditionally, this shift can be based in the understanding of three main topics: [10] [12]

- ***Process Dynamics:*** This topic relates to the dynamic response interrelationships between components (units) of a complex system, whose behaviour changes over time. Mathematically, they can be described by differential equations using either simple ideal models or more complex specific models for certain operations [10].
- ***Process Monitoring and Control:*** It is the field that studies all monitoring options and strategies of a process either manual or automatic. Its primary objective is almost always to make sure the process variables are maintained within desired operating conditions and parameters, safely and efficiently, while satisfying environmental and product quality requirements. Proper application of process control can improve the safety and profitability of a process [10] [13].
- ***Real time release testing (RTRT):*** RTRT is a system of release that gives assurance that the product is of intended quality, based on the information collected during the manufacturing process. Therefore, under specific circumstances an appropriate combination of process controls (critical process parameters) together with pre-defined material attributes provides greater assurance of product quality than end product testing [10] [12] [13].

According to FDA´s "Quality guidelines for Continuous manufacturing Guidance, 2019" [12] one of the most used and suitable scientific approach presented in this text to characterize how a material flows through the process is via the residence time distribution (RTD). The shape of the RTD reflects the degree of axial dispersion or back mixing within that system, which affects the propagation of disturbances, material traceability,and the control strategy (e.g., material diversion and sampling frequency). It is

important to understand how the RTD varies over the range of planned operating conditions as this information serves as a basis for material traceability and design of a control strategy [12]. Additionally, it is also reiterated the implementation of well-justified process monitoring approaches to develop a suitable control strategy. The utilization of PAT tools that generate real time information on process parameters and attributes of input materials and final product can enable high detectability of transient disturbances and process deviations, active process control and introduce real time release testing (RTRT) techniques [10] [11], where empirical or semi-empirical models can also be used as support options. For example, these models can include multivariate models to predict dissolution and calibration models associated with NIR procedures that are used for content uniformity [11] [13].

## 2.2 Polymers in the pharmaceutical Industry

The transition from batch to continuous has been widely explored from drug substance to drug product operations. Nevertheless, a widely used operation across the supply chain to support chemical and organic reactions, crystallization processes, purification, spray drying, and coating operations among others is solution preparation. Over the years the constant increase in demand for more specialized medicine as well as the high operating costs for solution preparation via batch have sparked the interest in addressing these problems by shifting the mode of the operation entirely. Nonetheless, the major challenges for preparing solutions in a continuous process are the material properties. Polymers are large molecules characterized by their insolubility and fouling tendency due to their natural stickiness and predisposition for the formation of foams and emulsions that cause them to adhere to vessel walls. In most applications the objective for the pair solute/drug is, for it to be dispersed within a polymer matrix and delivered to the intended target.Thus, applications for polymers in the pharmaceutical and medical field range from its use as coating agents and flavoured additives as excipients in drug formulation to tissue regeneration [14] [15].

According to Buckley *et al* (2007) [16] the most important uses of polymers are related to their physical state and the configuration of its chains which is defined by the interactions of the functional groups in the polymer chain and the medium where it is inserted. More specifically the importance falls back on whether a polymer is in its*amorphous* or *crystalline* state [17], thus:

***Amorphous state:*** This is defined as a physical state where the polymer chains are

randomly dispersed, coiled and interwinded with no molecular order or structure whatsoever.This concept can be further refined with glassy solids which are a specific case of amorphization where the solid is below a certain temperature threshold becoming fragile and brittle, the *glass transition temperature- $T_g$*. Here any solid, polymeric or not exhibits changes in its relaxation processes,thus below $T_g$, secondary relaxation processes, involving several contiguous groups along the chain cannot occur, causing the substance to become brittle and exhibit a glassy like behaviour. Above $T_g$ all types of relaxation processes,primary and secondary are present and are increasingly more intense according to temperature making so that in the case of polymers they exhibits a rubbery like behaviour and in extreme cases a viscous flow effect [18] [19].

***Crystalline state:*** On the other hand, crystallinity, is the packing of molecular chains to produce an ordered atomic array. Thus as a consequence of their size and complexity, polymer molecules are only partially crystalline (or semicrystalline), having crystalline regions dispersed within the remaining amorphous material. Any chain disorder or misalignment will result in an amorphous region, because twisting, kinking, and coiling of the chains prevent the strict ordering of every segment of every chain. Buckley *et al* (2007) [16] proposed that a semicrystalline polymer consists of small crystalline regions (crystallites), each having a precise alignment, which are interspersed with amorphous regions composed of randomly oriented molecules [14] [17].

One example where the entanglement of the individual chains is of the up most importance is in amorphous solid dispersions (ASDs), where the solid state form of the drug is changed from crystalline to amorphous (amorphization). The rationale behind this approach can be understood by the following equation [20]:

$$\Delta G_T{}^{Amorphous,Crystalline} = -RTln\left(\frac{\sigma_T^{Amorphous}}{\sigma_T^{Crystalline}}\right) \tag{2.1}$$

Here, $\Delta G_T^{Amorphous,Crystalline}$ is the energy difference between the crystalline and the amorphous state, R is the ideal gas constant, T is the absolute temperature of concern and $\sigma_T^{Amorphous}/\sigma_T^{Crystalline}$ is the solubility ratio between the two states [21] [20].

It follows from 2.1 that the amorphous form has a higher theoretical solubility as compared to the crystalline form due to its excess thermodynamic properties. In simple terms, in the amorphous state there is no energy requirement to break the crystal lattice structure so that the drug molecules can interact with solvent molecules through intermolecular interactions and become dissolved. However, the excess thermodynamic properties of amorphous forms also result in a natural tendency to crystallize thereby

negating the solubility advantage unless the structure is stabilized [21]. As a result, the onus falls back on manufactures to efficiently develop strategies to prevent crystallization

### 2.2.1 Polymer Solutions

In 1942 Gee and Treolar [22] reported that even dilute polymer solution deviated from idea-solution behaviour. As such, Paul Flory and Maurice Huggins [3] [1] proposed one of the oldest but still to this day widely accepted models for predicting polymer solution behaviour, *The Flory-Huggins Theory*, based upon a simple lattice model.

Accordingly, in low molecular weight compounds the lattice sites or holes of the compound molecular structure are the same size as the size of the solvent and therefore only one solute or solvent molecule can occupy a single lattice at a given time. The natural increase in the entropy of the system can then be estimated by statistc thermodynamics via the *Boltzmann Relation* (see equation 2.2) in order to explain the dissolution process.

$$\Delta S_m = kln\,(\Omega) \tag{2.2}$$

Where k is the Boltzmann constant and $\Omega$ is the total number of ways of arranging indistinguishable solvent and solute molecules and $\Delta S_m$ is the entropy gain of the system.

Nonetheless, when mixing a low molecular weight solvent with a high molecular weight polymer the entropy of mixing given by the equation 2.2 is lower than low molecular weight mixing. This is due to the loss in conformational entropy resulting from the linkage of individual repeating units along the polymer chain compared to the less ordered state of unassociated low weight molecules. In this case the lattice is divided in to *r segments* each of the size of the solvent molecule, where r is the ratio of polymer volume to solvent volume which as a result means that there is a lower total number of ways of arranging indistinguishable solvent and solute molecules.

In figure 2.1 lies a schematic representation of the theory.

As a result the Flory-Huggins theory postulated that instead of a polymer dissolving instantaneously and being controlled by the external mass transfer resistance through a liquid layer to the solid–liquid interface; the dissolution involves two transport processes: *solvent penetration and diffusion* through the polymer and *chain disentanglement*, where the chain change their conformation and prepare to disengage and diffuse from the polymer medium to the bulk solvent.

Narashma *et al* [2] established that when an uncrosslinked, amorphous, glassy polymer is in contact with a thermodynamically compatible solvent, causes a plasticising effect

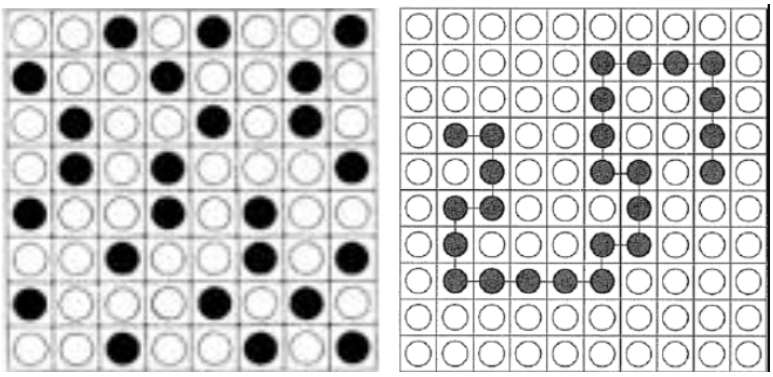

(a) (b)

**Figure 2.1:** Representation of two-dimensional Flory-Huggins lattice [1]:(a) Model for a low molecular weight solute in a solvent; (b) Model for a polymer chain in solution

(figure 2.2). As a result of the plasticizing effect, a gel-like swollen layer is formed along with two separate interfaces, one between the glassy polymer and gel layer and the other between the gel layer and the solvent. After an induction time,the polymer then dissolves.

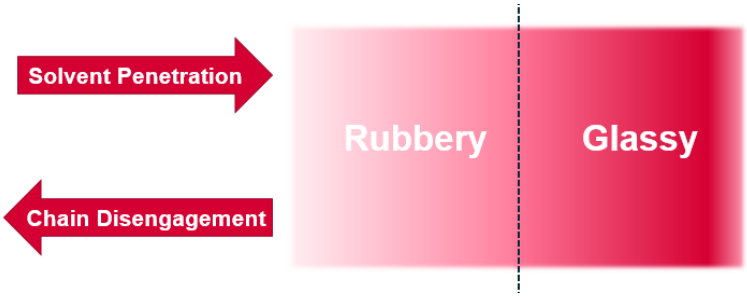


**Figure 2.2:** A schematic of one-dimensional solvent diffusion and polymer dissolution. (Adapted from Ref [2]

Other findings by Uberreiter [3] went on to not only explain in more detail how the dissolution occurs but also how to summarize the structure of surface layers. Accordingly, the solvent begins its aggression by pushing the swollen polymer substance into the solvent, and, as time progresses, a more dilute upper layer is pushed in the direction of the solvent stream. Further penetration of the solvent into the solid polymer increases the swollen surface layer until, at the end of the swelling time, a quasistationary state is reached where the transport of the macromolecules from the surface into the solution prevents a further increase of the layer.

The structure of the surface layers of glassy polymers during dissolution from the pure polymer to the pure solvent as it follows: the infiltration layer, the solid swollen layer, the gel layer, and the liquid layer (figure 2.3).

The infiltration layer is the first layer adjacent to the pure polymer. A polymer in

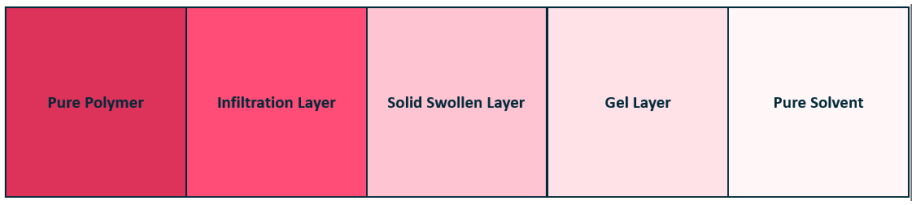


**Figure 2.3:** Schematic picture of the composition of the surface layer. (Adapted from Ref [3]

the glassy state contains free volume in the form of a number of channels and holes of molecular dimensions, and the first penetrating solvent molecules fill these empty spaces and start the diffusion process without any necessity for creating new holes. The next layer is the solid swollen layer where the polymer–solvent system building up in this layer is still in the glassy state. Next, the solid swollen layer is followed by the gel layer, which contains swollen polymer material in a rubber-like state, and a liquid layer, which surrounds every solid in a streaming liquid, respectively [23].

Despite the early stages this is the most widely accepted dissolution mechanism to present. However, there are still other authors who divide this theory into two approaches: one termed 'normal dissolution', where all of the layers described above are formed and the second type of dissolution when no gel layer is observed as it is refers in studies by Asmussen and Raptis; and Peckan *et al.* [24]

Additionally, over the year several polymer properties were found to be paramount to their dissolution, therefore we enumerate some of the key properties and discoveries in their respective fields.

**A-Effects of Molecular weight and polydispersity:** Cooper *et al.* [23] found that the dissolution rate decreases with increased polymer molecular weight in a non-linear behavior, additionally Manjkow *et al.* [22] discovered that poly-disperse samples dissolved about twice as fast as mono-disperse ones of the same $M_n$. Furthermore, Papanu *et al.* [25] established a critical molecular weight, where dissolution occurred by stress cracking, and proposed that the critical stress was dependent on molecular weight of the polymer. Lastly, Parsonage *et al.* [26] concluded that when the dissolution is controlled by chain disentanglement, which is a function of polymer molecular weight, larger molecular weights yield higher levels of disentanglement and thus have a higher degree of swelling before dissolution occurs.

**B-Effects of Stereochemistry and chain conformation:** Besides the molecular weight of the polymer, the dissolution process can also be affected by stereochemistry. Ouano and Carothers [27] found that the polymer dissolves either by exhibiting a thick swollen layer or by undergoing extensive cracking, depending on how fast the osmotic pressure

stress that builds up in the polymer matrix is relieved [28].

**C-Effects of different solvents:** Ouano and Carothers [29] [30] concluded that if the 'internal pressure' builds up faster than the glassy matrix can relax through gradual swelling, catastrophic fracture results. Also, they pointed out that polymer morphology at the molecular level has a strong influence on the kinematics of dissolution.Taking the previous studies further Cooper *et al.* [23] investigated poly(methyl methacrylate) (PMMA) dissolution rates with mixed solvents. The results showed that the addition of small non-solvent molecules to a good solvent resulted in a significant increase in the dissolution rate of PMMA films. This enhancement of the rate was proposed to be the result of 'plasticization' of the polymer films by the small, rapidly diffusing non-solvent molecules. Those molecules found to exhibit this enhancement effect at lower concentrations were water, methanol, and ethanol.

Lastly Harland *et al.* [28] focused their work in the swelling and dissolution of polymer for pharmaceutical and controlled release applications. They investigated the swelling and dissolution behavior of a system containing a drug and polymer and observed that the dissolution was characterized by two distinct fronts: one separating the solvent from the rubbery polymer and the second separating the rubbery region from the glassy polymer. The drug release had at 0:5 dependence relation to a diffusional term and a 1 relation to a dissolution term, and the drug release rate was independent of time when the two fronts' movements were synchronized.

**D-Effects of Process Conditions:** Uberreiter [1] found that the velocity of dissolution increases with the agitation and stirring frequency of the solvent due to a decrease of the thickness of the surface layer, and the dissolution rate approaches a limiting value if the pressure of the solvent against the surface of the polymer is increased (at all temperatures). Pekcan *et al.* [26] also studied the effects of agitation and found that with no agitation, the solvent molecules penetrate the polymer, and a gel layer forms. However, the gel layer decreases in magnitude with time due to desorption of the polymer chains. On the other hand, when agitation is present, no gel layer is formed because it is stripped off rapidly by the stirring process. In the later case, the sorption of solvent molecules is immediately followed by desorption of the polymer chains from the swollen gel layer.

### 2.2.2 Polymer Rheology

#### A-Newtonian Fluids

The viscous flow of Newtonian fluid is described by Newton´s law of viscosity given for shear flow as:

$$\tau = \mu \frac{\mathrm{d}\gamma}{\mathrm{d}t} \tag{2.3}$$

where $\tau$ i shear stress and $\mu$ is the Newtonian viscosity coefficient and $\frac{\mathrm{d}\gamma}{\mathrm{d}t}$ is the shear strain rate.

According to newton´s law the flow of substances can, thus be simply described as one which one of the three components of the velocity vector $u = (u_1, u_2, u_3)$ is non zero. An example of this simple shear flow is Couette shear flow between two infinitely wide parallel plates (figure 2.4). In this case $\gamma$ is defined as the ratio of deformation of a differential element in a direction, which mean that the the shear rate is equal to the velocity gradient:

$$\frac{\partial \gamma}{\partial t} = \frac{\partial}{\partial t}\left(\frac{\partial y}{\partial t}\right) = \frac{\partial}{\partial y}\left(\frac{\partial y}{\partial t}\right) = \frac{\partial u}{\partial y} \tag{2.4}$$

where $u$ is the velocity field in the x-direction. The maximum shear rate occur at the moving plate surface and is given as U/H, where U is the constant (maximum) velocity of the upper plate moving in the x direction and H is the maximum distance of the separation between the two plates.

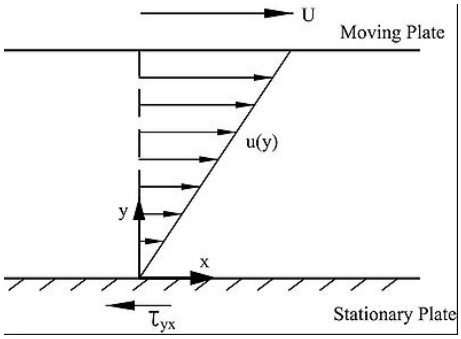


**Figure 2.4:** Newtonian Flow: Couette Flow with no pressure gradient

In Newtonian fluids $\mu$ is a function of temperature and pressure but is independent of $\frac{\mathrm{d}\gamma}{\mathrm{d}t}$.

**B-Non-Newtonian Fluids**

**Shear Rate dependence:** The Non- Newtonian or apparent viscosity($\eta$) of polymer solutions can also be defined through the general Newtonian fluid model, however the dependence of $\eta$ on $\dot{\gamma}$ (ratio of deformation) is given by the constitutive equation of the material.

$$\tau = \eta\left(\dot{\gamma}\right)\dot{\gamma} \tag{2.5}$$

Usually non-newtonian fluids have three characteristic regions. At low shear rates $\eta$ is nearly independent of $\dot{\gamma}$ and approaches a limiting zero shear rate value of $\eta_0$. At higher $\eta$, $\dot{\gamma}$ decreases with increasing. The fluids that exhibit this kind of behaviour are called shear thinning. (see figure 2.5)

**Figure 2.5:** Polymer Rheology:Shear-Thinning behaviour

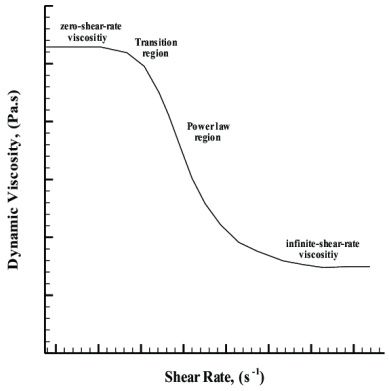


The molecular basis follows that at low shear values the entanglements impede shear flow and therefore viscosity is high. As shear rates increases the chains begin to orient in the flow direction and disentanglement from one another begins, the viscosity begins to drop. Finally when the molecules are totally oriented in the direction of the flow stable entanglements are no longer possible and the viscosity reaches a low value that is again independent on shear strain value. This second Newtonian plateau region is the defining characteristic of shear thinning polymer solutions, however when the opposite occurs and viscosity increases with shear rate we have a behaviour that is called shear thickening (Dilatants).

Nevertheless due to the distinct properties of polymer their behaviour is not always straightforward. Porfirio *et al* (2020) [31] investigated the rheological characterization of the most commonly used polymers and solvents to formulate amorphous solid dispersions. In their studies it was found that Copovidone solutions exhibit a Newtonian behavior whereas HPMC, HPMCAS and Eudragit L100 showed solvent-dependent non-Newtonian behavior. Additionally, HPMC and HPMCAS solutions showed shear thinning behavior and elasticity and, Eudragit L100 solutions showed a constant viscosity with elasticity, being therefore a Boger-like fluid [32] [33].

**Molecular weight dependence:** The significance of entanglements to shear thinning flow suggests that molecular weight and the critical molecular weight for entanglements should influence the rheological properties of polymers. The zero-shear viscosity, $\eta_0$ is directly related to the weight average molecular weigh average. In addition the onset of

shear thinning behaviour occurs progressively at lower $\dot{\gamma}$ as molecular weight increases [32].

**Temperature dependence:** The temperature follow a typical Arrhenius relationship at temperatures above $T_g$

$$\eta = \eta_r \cdot exp\left(\left[\frac{E}{R}\right] \cdot \left(\frac{1}{T} - \frac{1}{T_r}\right)\right) \tag{2.6}$$

where $\eta_r$ is the viscosity at some reference temperature. E is the activation energy and R is the ideal gas constant.

Nevertheless at lower temperatures in the vicinity of the glass transition temperature, viscosity increases much more rapidly with decreasing temperature than what is given by the Arrhenius equation. In this case one suitable approach is the WLF equation [33].

$$log\left[\frac{\eta\left(T\right)}{\eta\left(T_g\right)}\right] = log\left(a_t\right) = \frac{-C_1\left(T - T_g\right)}{C_2 + T + T_g} \tag{2.7}$$

where $\eta_{T_g}$ and $\eta_T$ are the viscosity at $T_g$ and a reference temperature $T$, respectively; and $C_1$ and $C_2$ are constants of type polymer melt that can be determined experimentally.

## 2.3 Material Tracking: Residence Time Distribution

CM or SCM has been recognized as an emerging technology by the US FDA for its potential to improve agility, flexibility, and robustness in pharmaceutical manufacturing. According to "FDA guidelines, 2019" [6] the importance of material tracking and the understanding of process dynamics to achieve reliable process performance to ensure acceptable product quality can be performed with residence time distributions (RTDs) [34].

Briefly described, a residence time distribution (RTD) is a diagnostic tool that characterizes the time a material resides inside of a unit operation. This technique is performed by introducing a traceable material (hereon referred to as the tracer) at a known position of a unit operation and then tracking the concentration of the tracer material as it exits the system. Differences in the RTD for various conditions can be used to determine the completeness of macro-mixing inside of a system as well as the characterization of mixing patterns with ideal or non-ideal mixing models [35].

Nevertheless, when considering the application of RTD methods, it is important to revisit the primary assumptions from which both experimental and mathematical understanding can be derived. The major assumptions and requirements provided by Danckwerts [36] and Nauman [37] [38] for the application of RTD as a characterization tool are listed below:

1. The system being studied is continuous (or semi-continuous) based on the addition and removal of components through streams with constant or intermittent flow.
2. The continuous (or semi-continuous) incoming and outgoing system flows have reached steady and equal values, indicating the system is now invariant throughout time or repeatable periods of time; i.e., either in a steady or a periodic state.
3. The inlet and outlet streams have unidirectional flows, so that once material and tracer enter the system it stays within the unit until it exits.
4. The addition of tracer materials does not affect the system's overall flow and the tracer is evenly distributed along the entire system's cross-section.

As such, two major scenarios are often observed with regards to acquiring RTD results: (1) diagnose phenomenological equipment behaviour and characterize mixing performance and, (2) understand the dynamic behaviour of upstream composition disturbances. The selection of tracer materials depends heavily on which of these two last scenarios is chosen, especially with regards to future application for model development. For example, if the goal is to establish the fate of a given amount of an ingredient entering the system (e.g., lump of API or excipient entering the system) for a particular formulation at fixed or ranging set of processing conditions (e.g., inlet flow rate, blade speed), then it is best to use that specific ingredient as a tracer to establish its RTD at the desired conditions [39] [40] [41] .

Therefore, from a tracer selection criteria, it is important to establish fundamental characteristics listed by Danckwerts for a good tracer. Consequently, a tracer must:

- Be detectable from other materials in the system.
- Be non-interactive with the system: a tracer ought not to be consumed, converted or transformed inside the equipment being studied nor should it affect the flow patterns inside of the system.If the tracer causes a change in the system, such change should be considered in the method that is being used.
- Have similar physical and flow properties to those of the system.

Lastly, for introducing tracer in the system there are two major methods: pulse (or impulse) and step change.

**Injection of tracer by impulse:**

Pulse or impulse experiments represent the precise and instantaneous introduction of an amount of tracer, $N_0$ into the feed stream of a reactor. Regardless of the type of tracer

addition, the resulting response of these experiments typically relies in the measurement of the outlet tracer concentration as a function of time. As such, for pulse experiments in a single-input and single-output system in which only flow (i.e., no dispersion) carries the tracer material across system boundaries the mathematical approach begins by choosing an increment of time $\Delta t$ sufficiently small that the concentration of tracer, $C(t)$, exiting between time t and $t+\Delta t$ is essentially the same. Therefore, the amount of tracer material, $\Delta N$, leaving the reactor between time t and $t + \Delta t$ is then calculated by equation 2.8:

$$\Delta N = C(t)v\Delta t \tag{2.8}$$

where $v$ is the effluent volumetric flow rate. In other words, $\Delta N$ is the amount of material exiting the reactor that has spent an amount of time between time t and $t + \Delta t$ in the reactor.Therefore, if it is divided by the total amount of material that was injected into the reactor, $N_0$ , it is obtained the following expression [41] [4]:

$$\frac{\Delta N}{N_0} = \frac{vC(t))}{N_0}\Delta t \tag{2.9}$$

which represents the fraction of material that has a residence time in the reactor between time t and $t+\Delta t$ and can then be used to define,for pulse injections the residence time distribution(E(t))so that:

$$E(t) = \frac{vC(t)}{N_0} \tag{2.10}$$

Where E(t) is the residence-time distribution function that describes in a quantitative manner how much time different fluid elements have spent in a reactor.

Additionally,if $N_0$ is not known directly, the residence time distribution function can be obtained from the outlet concentration measurements by summing up all the amounts of materials,$\Delta N$, between time equal to zero and infinity Therefore, since the volumetric flow rate, $v$ is usually constant we have [41]:

$$E(t) = \frac{C(t)}{\int_0^\infty C(t)dt} \tag{2.11}$$

The major difficulties with the pulse technique lie in the problems connected with obtaining a reasonable pulse at a reactor's entrance. The injection must take place over a period which is very short compared with residence times in various segments of the reactor or reactor system, and there must be a negligible amount of dispersion between the point of injection and the entrance to the reactor system. If these conditions can be

fulfilled, this technique represents a simple and direct way of obtaining the RTD [4] [41].

**Injection of tracer by step:**

Step changes, on the other hand, require the even, consistent, immediate, and continued introduction (positive step) or depletion (negative step) of a tracer. The resulting response out of a system with a step input is a distribution curve that begins at the initial value and ends at the tracer concentration set point. This latter point provides an advantage for detection methods (e.g., PAT tools) whose calibration and detectability are dependent on the original calibration method [42] [4].

As such, considering a constant rate of tracer addition to a feed that is initiated at time t=0 and considering that before this time no tracer was added to the feed the step injection of tracer can thus mathematically described by: [41]

$$C_0(t) = \begin{cases} 0 & t < 0 \\ C_0(constant) & t \geq 0 \end{cases} \tag{2.12}$$

Consequently. for cases when tracers are added using a step method, a differential distribution function – is calculated using the concentration of tracer at the system's outlet and the sum of that concentration over the whole time period. When tracers are added using step changes, a cumulative distribution function (CDF) is computed to perform the RTD calculations: [4]

$$F(t) = [\frac{C_{out}}{C_0}]_{step} \tag{2.13}$$

And by differentiation:

$$E(t) = \frac{d}{dt}[\frac{C_{out}}{C_0}]_{step} \tag{2.14}$$

Nevertheless,independent of the method used to determine the RTD researchers can derive two critical pieces of information about the system: the tracer's mean and distributed residence time. [4], from experimental data, the RTD can be characterized using the calculated mean residence time ($\tau$) and variance ($\sigma^2$ ). These can be determined using the following equations [4]

$$\tau = \int_0^\infty t \cdot E(t)dt \tag{2.15}$$

where t is the time stamp measured during the tracer experiment and E(t) correspond to the residence time distribution that was obtained experimentally.Accordingly, for the

variance we have:

$$\sigma^2 = \int_0^\infty (t-\tau)^2 \cdot E(t)dt \tag{2.16}$$

where $\tau$ is the mean residence time t is the time stamp measured during the tracer experiment and E(t) correspond to the residence time distribution that was obtained experimentally.

The increased involvement of RTD in the chemical engineering field has also led to the development of a myriad of models. However, the examples shown in this work use only ideal models such as the "stirred tanks in series" model, which is an empirical model based on equally sized continuously stirred tank reactors (CSTRs) placed in series and other ideal models like plug flow tubular reactor model (PFR). Nevertheless, the model for a CSTR assumes a mixed vessel with perfect back-mixing, however, it can used to model real reactor mixing by placing several CSTRs in series or in parallel as well as other convolutions between these two ideal models. Additionally, the plug flow reactor model can also be extrapolated by using a by an infinite larger number of tanks in series (see equation 2.17), resulting in an increasingly narrower distribution, which does not have any axial mixing and is represented by a step response [36].

$$E(t) = \frac{t^{n-1} \cdot e^{\left(\frac{-nt}{\tau}\right)}}{(n-1)!\left(\frac{\tau}{n}\right)^n} \tag{2.17}$$

where $\tau$ is the mean residence time and n is the number of continuous stirred tank reactors (CSTRs). Experimental data can be used to fit the parameters of this equation. Note that, the axial dispersion approach or any other methodology can be also use to develop the RTD model [36].

Additionally there also exists other expressions that allow for modeling plug flow reactors, such as 2.18 and the laminar flow model 2.19 [36].

$$E(t) = \frac{1}{\theta}\int_t^\infty \delta\left(t-\theta\right)dt \tag{2.18}$$

$$E(t) = \begin{cases} 0 & t < \theta \\ \frac{\theta^2}{2t3} & t \geq \theta \end{cases} \tag{2.19}$$

## 2.4 Process Monitoring

### 2.4.1 PAT tools

In this section, several PAT tools that can be used for monitoring a solution preparation are presented as well as a brief introduction to the technology.

***Refractometry***

Refractometry refers to the measurement of small changes in the refractive index of liquids and gases. Typically a refractometer determines the refractive index (symbolized as nD or RI) of a substance. This measurement allows for the characterization of the change in the speed of light beams when they travel across different mediums, due to the bending in the refraction angle. As such according to Snell's law of refraction, which states that the ratio of the sines of the angles of incidence and refraction is equivalent to the ratio of phase velocities in the two media, we can expect the the following through equation 2.20

$$n_1 sin(\theta_1) = n_2 sin(\theta_2) \tag{2.20}$$

Where $\theta_1$ and $\theta_2$ are the angles of incidence and refraction, respectively, of a ray crossing the interface between two media with refractive indices n1 and n2.

In figure 2.6 we have an illustration of the bending of the light

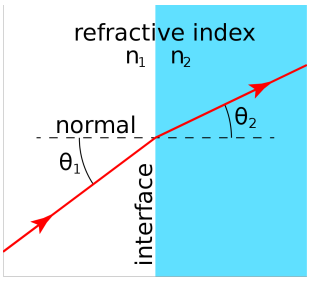


**Figure 2.6:** Refraction Index Background:Refraction of a Light ray

In polymer solution the same principle is applied nevertheless a in this case a thin layer of the liquid is placed between two prisms and the light source. Afterwords, the light is then shone through the liquid at incidence angles all the way up to 90°. A second prism is also present that has an index of refraction higher than that of the liquid, so that light only enters the prism at angles smaller than the critical angle for total reflection. Afterwards the critical angle is determined by according to Snell's law.

***Turbidity***

Turbidity is a technique to measure the appearance and disappearance of a solid in a solution or the overall surface of solid particles in a suspension.

Regardless of the methodology a turbidimeter measures the intensity of light passing through a sample, relative to a known initial light source, meaning that, it quantifies the amount of transmitted light remaining after scattering. When there is suspended matter in the light path, this naturally causes scattering and absorption of some light energy, which reduces the incident illumination falling on the photodetector thus allowing for turbidity measurements. The source–detector relationship can vary widely between instruments and is often cited as the key reason to explain the different readings obtained on the same sample by different devices.

There are several units of turbidity measurement, with different measurement standards. Some of the most common measurement units are Formazin Turbidity Unit (FTU) and Nephelometric Turbidity Unit (NTU).

***Viscosity***

Perhaps when considering polymer technologies and polymer processes, viscometry is one of the most important techniques. Typically, viscometers measure the fluid viscosity by one (or a combination) of two principles:

1. Exposing a constant-area moving surface to a constant thickness of fluid a measuring the forces that resist the movement of the surface;

2. Exposing a constantly moving thickness of fluid to a fixed surface and measuring the forces that resist the fluid flow.

Thus, Capillary flow,falling body, orifice-type and paddle viscometers are more suited to measuring Newtonian fluids or fluids in a stationary position, whereas rotational- and vibrational- viscometers are more suited for in-process measurement and to measure non-Newtonian fluids. Polymeric solution behaviour depends on the polymer used: Newtonian behaviour is shown with copovidone solutions whereas HPMC and HPMC-AS solutions display a non-Newtonian behavior. Thus, vibrational viscometer is the most suitable process viscometer to be used in both types of fluids, Newtonian or non-Newtonian Vibrational viscometers consist of a probe inserted into a solution to which a vibrational force is applied. When comparing the different types of vibrational viscometers, O'Shea *et al.* (2019) [33] found that torsional vibration performed the best.

***NIR-spectroscopy***

NIR is a region of the electromagnetic spectrum that has unique properties which make it very useful for characterizing materials. The NIR region is from 700 to 2500 nm.

This area of the electromagnetic spectrum has the best combination of attributes for the analysis of most solid, slurry and liquid samples.

In this region the electromagnetic radiation interacts with OH, NH and CH bonds and certain wavelengths (frequencies) are associated with each bond type. When NIR light is presented to samples high in chemical compounds containing these bonds, some of energy is absorbed by the sample in these specific wavelengths, and thus the reflected light has less intensity in these regions. The differences in the reflected signal (spectrum) can be correlated to chemical concentration differences, and this forms the basis of an NIR calibration. Once this calibration is established, it can be used to predict the chemical concentration of unknown samples.

As an example, proteins are characterized by the presence of NH bonds found in the individual amino acids. The NH bonds absorb NIR radiation in multiple regions across the NIR spectrum at various levels. The more protein in the sample, the more energy that is absorbed in these region and the reflected energy has less intensity in this region. Calibrations can be developed which define the relationship between the NIR spectrum of a sample and constituent of interest, and these calibrations are then used in routine use to analyze new samples.

***Ultrasonic Spectroscopy***

Ultrasonic spectroscopy is a spectroscopic technique for material analysis utilizing high-frequency acoustical (ultrasonic) waves (frequency greater than 100 kHz). The two main parameters measured in ultrasonic spectroscopy are the velocity (m/s) and the attenuation ($s^2/m$) of the sound waves.

The ultrasonic velocity is determined by the density and adiabatic compressibility (elasticity) of the medium it travels through. It is very sensitive to intermolecular interactions and composition of the sample (e.g., particle size and density).

Ultrasound measurements are typically employed in crystallization processes for the determination of solubility points, metastable zone width and crystal growth rates. Since said process parameters are functions of concentration, they can be quantified using ultrasound technique. Additionally they can also be used to detect solvent-mediated phase transitions due to changes in sonic velocity when the composition of the solution changes. However, the measurement of ultrasonic velocity is significantly influenced by both temperature and moisture; and by process conditions, such as high air/gas bubble content and turbulence due to a high pump stroke, which can cause a reduction in the ultrasonic velocity and lead to high fluctuations or even loss of the measurement signal

### 2.4.2 First Principles Dissolution Models

Over time several models have been formulated to explain dissolution behavior however regardless of the approach there are five main ways of modeling amorphous polymer dissolution:

1. Phenomenological models with Fickian equations: These models attempt to physically describe the dissolution process using Fickian conditions and the moving boundaries present in the system.

2. Models with external mass transfer as the controlling resistance to dissolution. These models assume that the controlling factor in dissolution is resistance due to an external mass transfer.

3. Stress relaxation models and molecular theories: These models predict the polymer relaxation response to solvent uptake.

4. Analysis using transport models for swelling and scaling laws for chain disentanglement: These models are used to calculate polymer dissolution in the anomalous transport and scaling models.

5. Continuum framework models: These take into account the viscoelastic effects and mobility changes of the polymer during dissolution while using anomalous transport models to predict the behavior of solvent diffusion.

Figure 2.7 presents some of the primary models for polymer dissolution according to what was mentioned above.

**Figure 2.7:** First principle polymer Dissolution models and their constraints and assumptions

| Model Name | Type of Model | Assumptions | Model equations | References |
|---|---|---|---|---|
| **Vrentas & Vrentas (1998) Rubbery Dissolution** | External complex mass transfer | • Completely miscile binary mixture of solvent and polymer.<br>• Limiting step solvent diffusivity through the polymer<br>• There is no external induced flow that changes the diffusion field | $\frac{\partial C_p}{\partial \tau} = \frac{d}{d\lambda}\left(\frac{D}{D_s}\frac{\partial C_p}{\partial \lambda}\right)$<br>Where cp is the polymer concentration, τ-dimensionless time,λ-scale length, D/Ds-dimensionless diffusivity | Vrentas JS, Vrentas CM. Dissolution of rubbery and glassy polymers. J Polym Sci, B, Polym Phys 1998;36(14): 2607–14. |
| **Vrentas & Vrentas (1998) Glassy Dissolution** | External complex mass transfer | • Completely miscible binary mixture of solvent and polymer. Limiting step solvent diffusivity through the polymer<br>• There is no external induced flow that changes the diffusion field<br>• **Solvent diffusivity varies with concentration** | $\frac{\partial C_p}{\partial \tau} = \frac{d}{d\lambda}\left(\frac{D}{D_s}\frac{\partial C_p}{\partial \lambda}\right)$<br>$kC_p \geq 0, \quad \frac{D}{D_s} = exp(-kC_p)$<br>Where k is a model parameter for concentration dependence of diffusivity. | Vrentas JS, Vrentas CM. Dissolution of rubbery and glassy polymers. J Polym Sci, B, Polym Phys 1998;36(14): 2607–14. |
| **Devota et all (2014)** | Disengagement Dynamics | • Polymer particles are placed in a uniform stream of moving solvent with velocity v.<br>• Solvent penetration in not uniform in the particle.<br>• **Chain disengagement is the limiting step in polymer dissolution** | $\alpha\left(\frac{\partial \varphi_p}{\partial t}\right) + \frac{1}{r^2}\frac{\partial}{\partial r}(r^2\varphi_p v_r) + \frac{1}{r\sin\theta}\frac{\partial}{\partial \theta}(\sin\theta\,\varphi_p v_\theta) = \frac{1}{Pe}\left[\frac{1}{r^2}\frac{\partial}{\partial r}\left(r^2 D_p v_t \frac{\partial \varphi_p}{\partial r}\right) + \frac{1}{r^2\sin\theta}\frac{\partial}{\partial \theta}\left(\sin\theta\, D_p \frac{\partial \varphi_p}{\partial \theta}\right)\right]$<br>Where vr and vθ are the velocity components of the field and Pe is the peclet number | Devotta I, Ambeskar VD, Mandhare AB, Mashelkar RA. The lifetime of a dissolving polymeric particle. 2014 |
| **Multi stephan phase (1977)** | Fickian Transport model | • Constant chain dissociation during dissolution<br>• Sharp changes in the two boundaries formed in the polymer (rubbery and glass).<br>• **Process is dissociation controlled** | $\left(\frac{\partial \varphi_s}{\partial t}\right) = \frac{1}{r^2}\frac{\partial}{\partial r}\left(r^2 D_s \frac{\partial \varphi_s}{\partial r}\right) - \left[\frac{1}{r^2}\frac{\partial}{\partial r}(r^2 v_s \varphi)\right]$<br>Where vs is the swelling velocity of the polymer particle and Ds is the difusivity of the solvent into the polymer | Tu Y-O, Ouano AC. Model for the kinematics of polymer dissolution. IBM J Res Develop 1977; 21(2):131–42. |

### 2.4.3 Sensor Fusion and Soft sensors

Despite its numerous applications one common trend in the pharmaceutical industry is the idea of sensor fusion, according to Lin *et al* 2017 [43], this idea transcends from the conventional control options and allows for soft sensors can be developed following a model-based approach, in which first principles models together with real time data are applied to describe the dynamics of the system. However, in order to successfully follow such an approach, it is necessary to have a deep understanding of the process at hands, as well as accurate approximations of all the parameters involved [44]. Furthermore this concept of Sensor Fusion has been widely applied in areas like autonomous vehicles, smart healthcare, precision farming and smartphones for better decision making [45].

While the advantage of these instrumental quantification is obvious as it usually produces high accuracy data, the disadvantages such as long turnaround time and low sampling frequency can often lead to inefficient process monitoring and control. Therefore, to obtain more frequent and faster estimations of product quality variables, software sensors (also known as soft sensors or inferential sensors), including partial least squares (PLS) models [46] [8] [47] and other data-driven mathematical models like neural networks or kalman-filter algorithms, have been widely applied over the past three decades. Hence, combining these available information from software and hardware sensors using sensor fusion is an attractive option to enhance the accuracy and reliability of process monitoring. With the use of sensor fusion, the assets of industrial chemical processes will be operated in a more efficient, reliable and profitable manner [48] [49].

Application examples of the aforementioned soft sensors include the use of PLS-calibrated models from spectroscopic data to estimate the concentration of the API in real-time [50] [7], to estimate the powder density of a pharmaceutical formulation in real-time [51], to identify critical quality attributes for real-time release [52], and for particle segregation assessment [53].

# 3

# Materials and Methods

## Contents

3.1 Materials . . . . . 28

3.2 Methods . . . . . 30

## 3.1 Materials

In this section it is presented the raw materials as well as the equipment that was used during the experimental work.

In this work it was used four different types of polymers and grades: HPMC grade E5 (Dow Chemical Company, USA), HPMC-AS grade MG (Shin-Etsu Chemical Co., Ltd., Japan) Copovidone (Kollidon VA64, BASF, Germany), and Eudragit L100 (Evonik Industries, Essen, Germany). In figure 3.1 lies a brief description of the raw polymers used, with some of their key and unique properties, observations and applications.

Additionally, all the polymers described above from this point on will be referred as $P_1$,$P_2$ $P_3$ and $P_4$ under no specific order. The corresponding nomenclature can be seen in appendix A.1

Additionally, both deionized water and organic solvents were also used in this work, more specifically it was used dichloromethane (Drogas Vigo, SA, Porriño, Spain), acetone (Drogas Vigo, SA, Porriño, Spain), and methanol (Bresfor – Indústria do Formol, S.A., Portugal). The selected combinations of polymer-solvent pairings aims to enable the proof of concept for the present work as they can be considered case studies of the process. As such, their choice, was selected based on their applications, company background and overall usefulness for processes that use polymeric solutions during drug formulation (e.g. wet granulation, coating, spray-drying, etc...).

| Polymer | Applications | Structure | Grades | Solubility | Rheology | Manufacturing |
|---|---|---|---|---|---|---|
| **HPMC**-(partly Omethylated and O-2-hydroxypropylated cellulose) | • Binder<br>• Film Coating agent<br>• Polymer matrix | 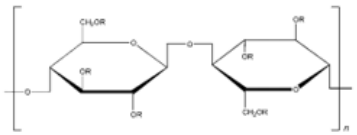 <br>where R is H, $CH_3$, or $CH_3CH(OH)CH_2$ | Grades may be distinguished by appending a number indicative of the apparent viscosity, in mPa s, of a 2% w/w aqueous solution at 20°C | Soluble in cold water, practically insoluble in chloroform, and ethanol, but soluble in mixtures of ethanol and dichloromethane, mixtures of methanol and dichloromethane, and mixtures of water and alcohol. ** | HPMC exhibits a non-Newtonian shear thinning behaviour | Cellulose reacts with sodium hydroxide to produce a swollen alkali cellulose. The product is then treated with chloromethane and propylene oxide to produce methyl hydroxypropyl ethers of cellulose. |
| **HPMC AS** – (mixture of acetic acid and monosuccinic acid esters of hydroxypropylmethyl cellulose) | • Binder<br>• Film Coating agent<br>• Polymer matrix | 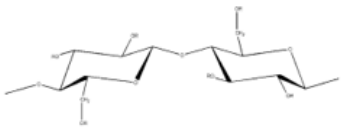 <br>Where -OR represents one of the following functional groups -hydroxyl, methoxyl, 2-hydroxypropoxyl, acetyl, or succinoyl. | Available in grades according to the pH at which the polymer dissolves (low, L; medium, M; and high, H), which vary in extent of substitution of acetyl and succinoyl groups, and in particle size, F (fine) or G (granular). | Practically insoluble in ethanol (95%), hexane and xylene. HPMC AS can be dissolved in buffers of pH greater than 4.5 with the rank order of solubility for the various grades increasing with the ratio of acetyl over succinoyl substitution. | HPMC-AS exhibits a non-Newtonian behaviour with increasing shear rate, particularly a shear-thinning behavior.54 | HPMC AS is produced by the esterification of hypromellose with acetic anhydride and succinic anhydride, in a reaction medium of a carboxylic acid. |
| **Copovidone**-( Acetic acid ethenyl ester, polymer with 1-ethenyl-2-pyrrolidinone) | • Binder<br>• Film Coating agent<br>• Polymer matrix<br>• Film forming agent | 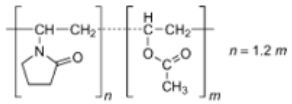 <br>$n = 1.2\ m$ | (Not applicable) | Greater than 10% solubility in butane diol, chloroform, dichloromethane, ethanol (95%), methanol, propanol, and water. Less than 1% solubility in cyclohexane, diethyl ether, liquid paraffin, and pentane | Copovidone solutions exhibit Newtonian behaviour. | Copovidone is manufactured by free-radical polymerization of vinylpyrrolidone and vinyl acetate in a ratio of 6: 4. The synthesis is conducted in an organic solvent |
| **Eudragit L100**-( methacrylic acid–ethyl acrylate copolymer (1 : 1) as a copolymer of methacrylic acid and ethyl acrylate) | • Transdermal delivery systems<br>• Film coating agents<br>• binders | 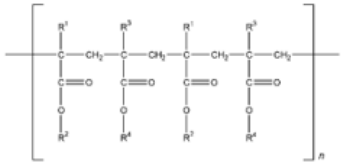 | (See Below) | Soluble in acetone and alcohols, but insoluble in dichloromethane, ethyl acetate, water and petroleum ethers | Solutions are considered Boger fluids, with constant viscosity and elasticity | Prepared by the polymerization of acrylic and methacrylic acids or their esters, e.g. butyl ester or dimethylaminoethyl ester. |

**Figure 3.1:** Summary of the polymers used and their properties/applications

## 3.2 Methods

The Methodology used following for the experimental polymer dissolution tests were performed according to Vitor Hugo Pereira´s Dissertation for Master of Science in Pharmaceutical Engineering, University of Lisbon "Exploring Process configurations and PAT tools in solution preparation" [54], where as the necessary equipment and methodology were upgraded in order to respond to the necessities of the work. For further details in this subject we suggest reading appendix A.2.

Additionally the PAT tools used throughout this work are described hereafter:

*Viscometer* - A vibrational viscometer (ReactaVisc 300, Hydramotion Ltd, England) was used for the continuous on-line measurement of fluid viscosity. This equipment has no moving parts, set list or bearings, and can be mounted in any vessel of suitable dimensions fitted with an appropriate connector or adaptor. The equipment as an adjustable time sample parameter that enables the user to predetermine sampling time ( 1s, 5s, 10s and 1 minute), in this particular case it was defined for the probe to measured the viscosity every 5 seconds in order not to overload the recording software. The probe also has a built-in temperature sensor.

**Figure 3.2:** Hydramotion vibrational viscometer

For viscosity measurements the sensor element consists of a resonant structure with an end cylinder (or "bob",), which vibrates at a specific frequency. When vibrating the bob shears through the fluid, energy is lost to the drag forces on the bob surface caused by the viscosity of the fluid and the loss of energy is used to determine the actual viscosity of the fluid.

*Refractometer:*An inline process refractometer (PR- 23, K-Patents Oy, Finland) was used for measuring liquid concentrations in process. This measurement was based on the refraction of light in the process medium.

*Turbidimeter:* A ratio turbidity sensor (TF16-N + C4000, optek-Danulat GmbH, Germany) coupled to a photometric converter was used. The sensor is a dual channel scattered light turbidimeter, designed for direct installation into pipelines, allowing for inline real-time process monitoring. It uses near-infrared light from 730 to 970 nm to measure solids concentration independent from color changes and assess the dissolution end-point.

# 4

# Process Dynamics and Modeling

## Contents

4.1 Process Dynamics: Residence Time Distributions . . . . . 32

4.2 Polymer dissolution Models . . . . . 38

## 4.1 Process Dynamics: Residence Time Distributions

Residence time distribution (RTD) models are essential to understand process dynamics and support process monitoring and control in continuous manufacturing systems. RTD models can also be used to monitor material traceability and to isolate intermediate materials or finished products when specifications are not met.

### 4.1.1 Methodology

When considering the application of RTD methods for equipment characterization, it is important to revisit the primary assumptions from which both experimental and mathematical understanding can be derived. The major assumptions and requirements provided by Danckwerts [36] and Nauman [37] [40] for the application of RTD as a characterization tool are the following:

1. The system being studied is continuous (or semi-continuous) based on the addition and removal of components through streams with constant or intermittent flow.

2. The continuous (or semi-continuous) incoming and outgoing system flows have reached steady and equal values, indicating the system is now invariant throughout time or repeatable periods of time, either in a steady or a periodic state.

3. The inlet and outlet streams have unidirectional flows, so that once material and tracer enter the system it stays within the unit until it exits, never to return.

4. The addition of tracer materials does not affect the system's overall flow and the tracer is evenly distributed along the entire system's cross-section. Although observer effects are expected when studying any system, this last assumption aims at reminding experimenters to minimize this error.

Based on literature sources when RTD has been used in pharmaceutical applications, two major scenarios are often observed [38] [39]:

1. Diagnosis of phenomenological equipment behavior and characterization of mixing performance

2. To understand the dynamic behavior of upstream composition disturbances as they travel through the process for a particular formulation and/or train of unit operations.

Although these two scenarios are closely tied, the latter is more closely related to a specific process and formulation (i.e., set of material properties) while the first focuses on describing the equipment's intrinsic behavior irrespective of a particular formulation, meaning that it aims at considering the effect of material properties on the measurement. For example, if the goal is to understand the dynamics and the trajectory of a given amount of an ingredient entering the system (e.g., lump of API/ polymer or tracer entering the system) for a particular formulation at fixed or ranging set of processing conditions (e.g., inlet flow rate,blade speed), then it is better to use that specific ingredient to establish its RTD at the desired conditions.

Therefore, in this work it is necessary to revisit some of the RTD´s fundamentals with respect to tracer selection. The fundamental characteristics listed by Danckwerts [36] for a good liquid tracer are that they must:

- Be detectable from other materials in the system.
- Be non-interactive with the system: a tracer ought not to be consumed, converted or transformed inside the equipment being studied nor should it affect the flow patterns inside of the system. If the tracer causes a change in the system, such changes should be carefully assessed and special conditions should be defined.
- Have similar physical properties to those of the system:similar flow properties to those in the system.
- Be able to mix with other system components: similarly to the previous point, the material should be able to traverse the equipment interacting in a similar fashion as the other components.

**Process Conditions for using polymer tracer in polymeric systems**

The idea of using polymer as tracers came from not only recommendations in the literature but also as convenience factor in the understanding of the dynamics and the fate of a given amount of an ingredient entering the system. Therefore in accordance with the literature [4] two major conditions need to be met when measuring RTDs in polymeric systems for them to be used:

1. Tracer concentration must be such that it must not affect the hydrodynamic behaviour of the system.
2. Any phenomenon occurring in the system must be considered instantaneous to not change the global hydrodynamics of the process.

Taking into account the previous conditions available in the literature and considering basic chemical engineering knowledge in order to sustain these conditions, for the dissolving polymer to be used as a tracer in the existing system, the following assumptions were proposed:

1. The ratio of inertial forces to viscous forces that the fluid is subjected to, in relatio internal movement due to different fluid velocities must be constant throughout the dissolution process. This means that the Reynolds number must be constant throughout the dissolution process (Upper and Lower must be such that $Re(t) < 10\% of Re_0$) [41].
2. Global dissolution time of the polymer in the system must be considered instantaneous and therefore should be lower than the experimental obtained mean residence time.

In order to summarize the key aspects of using dissolving polymers as tracers to obtain RTDs experimentally a schematic representation of the approach that was used to verify the hypothesis:

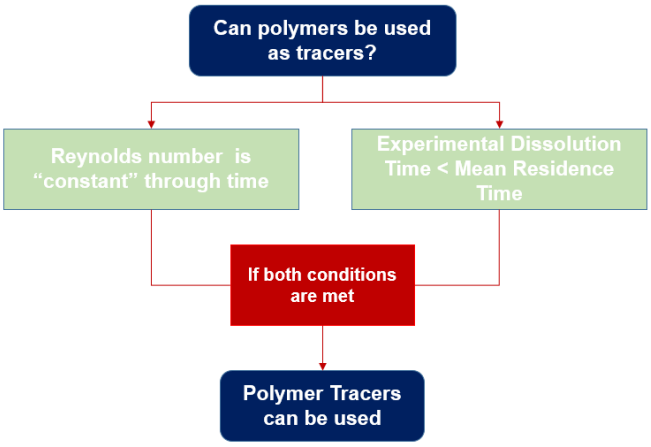


**Figure 4.1:** Schematic representation of the conditions required for Polymers to be used as tracer in the existing systems. Adapted from [4]

Considering this approach each solvent:polymer pair will actively define a system itself and present unique results.

### 4.1.2 Consistency Tests

Another important topic when determining RTDs experimentally is the evaluation of the consistency of the results. For example, dead volume and preferential paths can be easily determined with only the experimental results. These operational problems can be easily

verified by two tests called consistency tests which aim to verify the consistency of the data collected assuming the tracer´s choice has no influence in the flowing pattern of system. Therefore the two types of tests performed were the following [39] [41]:

1. Comparison between the amount of tracer that was injected and the total amount that was detected at the exit of the reactor

$$\frac{N_s(t)}{Q} = C_0 \int_0^t E(t')dt' \tag{4.1}$$

   Where $Q$ is the flow rate during operating conditions, $C_s$ is the outlet tracer concentration and and $C_0$ is the initial tracer concentration also detected at the outlet of the reactor.

2. Comparison between the average residence time$\bar{t}$ obtained experimentally from the values of E(t) and the corresponding value based on the volume and flow rate that were used in the trials.

$$\bar{t} = \int_0^\infty t \cdot E(t)dt \tag{4.2}$$

If both consistency tests are satisfied then the reactor is operating under ideal conditions, however if the opposite occurs or if one of tests is not verified the reactor presents either both preferential paths (by-pass) and dead volume or only one of the problems mentioned.

Additionally the dead volume and the by pass flowrate can be estimated according to the following expressions.

$$\frac{N_s}{N_e} = \frac{Q_e}{Q} \tag{4.3}$$

Where $Q_e$ is the effective flow rate during operating conditions, Q is the feed flowrate and $N_s$ and $N_e$ are the outlet and inlet tracer quantities respectively. Therefore the amount of dead volume can be determined:

$$\bar{t} = \frac{V_e}{Q_e} = \frac{V - V_{dead}}{Q_e} \tag{4.4}$$

Where $\bar{t}$ is the mean residence time obtained experimentally, $Q_e$ is the effective flow rate during operating conditions and $V_{dead}$ is the amount of dead volume and V is the volume of the reactor

### 4.1.3 Real Reactor Modeling based on Ideal reactors

For the real reactor modeling of the existing systems, the RTD experimental data was fitted to several ideal flow models using a least squares curve fitting approach based on the region-reflective algorithm described by Coleman *et al* [38]. The modeling of the experimental results was performed for ideal CSTR behaviour as well as Plug flow, Laminar flow and some convolutions between these models either in series or in parallel. For each respective model the concentration profile defining parameters ($C_0$, $\tau$, and n) for each respective model were determined by this least squares technique, which seeks these values while minimizing the sum of square (SS) error between estimated and experimental values:

$$SS = min_X \sum_i \left(C\left(X, t_i\right) - C_i\right)^2 \tag{4.5}$$

where C(X,ti) is the estimated concentration, $t_i$ and $C_i$ represent the $i^{th}$ points from the experimentally collected time and concentration datasets, and X is the parameter set for the models: $X = [C_0; \tau; n]$. When considering models such as laminar flow n=0

**Convolutions**

Regarding convolutions and despite knowing the RTD for the ideal basic models (Plug flow reactor-PFR, Continuous stirred tank reactor-CSTR, and Laminar flow reactor - LFR) , it is important to see how RTDs are obtained for any association of reactors either in parallel or in series. Traditionally this is obtained through the mass balance to all the reactors when a pulse like addition of tracer is used. Nevertheless, if the system response is linear and if the RTD of the individual ideal reactors are known (i.e., if the tracer does not modify the flow properties of the blend), any point in time will behave and spread through the system equally and thus convolution integrals can be used for combing multiple ideal RTD models. Therefore, it is presented the generalized way of determining the RTD of an association of ideal reactor either in parallel or in series [38] [40].

- For association of two arbitrary reactors in series with known RTDs (see figure 4.2 ) we have the following rationale:

Since there are the two reactors associated in series, we do not know how a certain volume element at the reactor outlet with time, $t$, has divided its time between the two reactors. As such there are countless possibilities, ranging from the fact the tracer may have spent 0 units of time in the first reactor and $t$ in second reactor. Nevertheless if the RTDs of the reactors are known, the probability of each of these occurrences can be

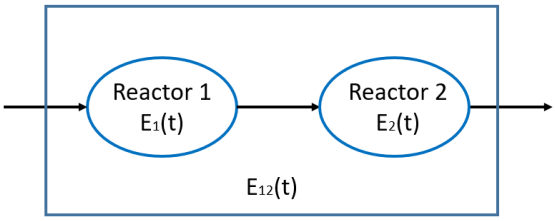


**Figure 4.2:** Association of Reactor in series with know RTDs

calculated since $E(t)$ is a probability function. Therefore, the probability of a volume element having spent $t'$ units of time in the first reactor and $(t - t')$ in the second can be calculated through the convolution equation of the $E(t)$ of both probability functions, $E_1(t')$; $E_2(t - t')$.

$$E_{12}\,(t) = \int_0^t E_1\,(t')\,E_2(t' - t)dt' \tag{4.6}$$

Another possibility for the global RTD determination comes from the fact that the number of volume elements that leave the system at a residence time t is given by the product between the number of control elements that leave the first reactor with a time t' by unit of time, $QE_1(t')dt'$ and the fraction of control elements that pass trough the second reactor with a time $(t - t')$ and $QE_2(t - t')dt'$.

$$QE_{12}\,(t)\,dt = \int_0^t QE_1\,(t')\,dt' E_2(t' - t)dt' \tag{4.7}$$

Where Q is the flow rate that the reactor is subjected to

Additionally for determining the outlet concentration of tracer the following equations can be used:

$$C_{out}(t) = \int_0^t C_{in}(t') * E(t')dt' \tag{4.8}$$

And for an association of reactors

$$C_{out}(t) = \int_0^t C_{in}(t - t')E(t')dt' = \int_0^t C_{in}(t')E(t - t')dt' \tag{4.9}$$

Moreover for a discretization for multiple reactors in series we have the following definition:

$$E(t_k) = \sum_j E_1(t_j)E_2(t_k - t_j + \Delta T)\Delta T) \tag{4.10}$$

where ΔT is the time interval for the two RTDs and $t_k$ and $t_j$ are the $k^{th}$ and $j^{th}$ points of the existing time array. This generalized response can then be applied countless times and to any type of ideal model that can be tested.

- For and association of reactors in parallel

On the other hand when considering an association of rectors in parallel the number of control volume elements that leave with time t by unit of time ( $QE_{12}(t)dt$) will be the sum of the control elements that spend time t in each of the reactors ($QE_1(t)dt$) and ($QE_2(t)dt$). Therefore we have he following equation:

$$QE_{12}\left(t\right)dt = Q_1E_1\left(t\right)dt + Q_2E_2\left(t\right)dt \tag{4.11}$$

Where $Q_1$ and $Q_2$ and the flow rates that pass trough each reactor, with $Q = Q_1 + Q_2$. The global RTD of a parallel association of reactors will therefore be the sum of the RTDs of each reactor weighted by the fraction of flow rate that passes trough each one.

Consequently, by generalizing an infinity array of parallel rectors we have:

$$E(t_k) = \sum_j E_1(t_j + \Delta T) + E_2(t_k - t_j + \Delta T)) \tag{4.12}$$

Therefore, in the present work this approach was subjected to 3 types of systems, battery of CSTRs, plug flow+Battery of CSTRs, plug flow in series and laminar flow + CSTR.

## 4.2 Polymer dissolution Models

Regarding polymer dissolution models the present work tested two models: Vrentas Vrentas (1998) and Devota *et al* (2014)

### 4.2.1 Vrentas and Vrentas (1998) Model

In the model proposed by Vrentas and Vrentas(1998) both the lack of moving boundaries in the diffusion field coupled with the solvent penetration and disentanglement of polymer chains phenomenon cause the overall dissolution process to be considered part of a complex diffusion process involving polymer and solvent in a single phase.Therefore, for the dissolution of either rubbery or glassy polymers, the species continuity equation is expressed as: [55] [56]

$$\frac{\partial C_p}{\partial \tau} = \frac{\partial}{\partial \lambda}\left(\frac{D}{D_s}\frac{\partial C_p}{\partial \lambda}\right) \tag{4.13}$$

Where, $C_p$ is the dimensionless polymer concentration, $\tau$ is the dimensionless time, and $\lambda$ is the dimensionless length scale. Also the dimensionless variable can be obtained through the following equations:

$$\lambda = \frac{r}{r_0} \tag{4.14}$$

$$C_p = \frac{\rho_p}{\rho_s} \tag{4.15}$$

$$\tau = \frac{D_s t}{r_0^2} \tag{4.16}$$

In the case of the rubbery dissolution the concentration profile can be determined by modeling the diffusion coefficient of the solvent into the gel-like part of the polymer ($D_s$) and the particle radius ($r_0$) [55] [57].

In the case of a glassy dissolution the difference resides in the strength of the concentration dependence of the two cases therefore an exponential concentration dependence of the mutual diffusion coefficient that is expressed as follows is introduced as a model parameter.

$$\frac{D}{D_s} = exp\,(k \cdot C_p) \tag{4.17}$$

For the glassy dissolution approach there is an additional parameter to be modeled, k that represents this concentration dependence in addition to the particle radius and solvent difusivity into to the polymer [57].

### 4.2.2 Devota *et al* (2014) Model

On the other hand, the model proposed by Devotta *et al* (2014) states that we can predict the lifetime of dissolving polymeric powders in a hydrodynamic field by including the phenomenon of reptation of the polymer chains, disengagement of these chains from the gel–liquid interface, and, also, diffusion in the boundary layer surrounding the gel–liquid interface. In this model the minimum time for a polymer to reptate out of the entangled swollen network and disengage itself from the interface is assumed to be equal to the reptation time, $t_{rep}$, which is primarily dependent on the structure of the polymer and

molecular weight. Additionally, since polymer chains, are long and mutually entangled, they are also inhibited from entering the liquid phase due to the dynamic friction between the chains. It was proposed that the rate at which the polymer chains disengage themselves from the gel–liquid interface is one of the factors controlling the dissolution rate in polymeric systems and if the dissolving polymer particles are placed in a uniform stream of solvent moving with velocity $v_1$;then the polymer concentration field will not be uniform in the r and u directions leading to the following equation for the determination of concentration profile in the medium [58] [59].

$$\frac{\partial C_p}{\partial t} + \frac{1}{r^2}\frac{\partial}{\partial r}\left(r^2 v_r C_p\right) + \frac{1}{sin\theta}\frac{\partial}{\partial \theta}\left(sin\theta v_\theta C_p\right) = \\ = \frac{1}{Pe}\left[\frac{1}{r^2}\frac{\partial}{\partial r}\left(r^2 D_p \frac{\partial C_p}{\partial r}\right)\right] \\ + [\frac{1}{r^2 sin\theta}\frac{\partial}{\partial \theta}\left(sin\theta D_p \frac{\partial C_p}{\partial \theta}\right) \tag{4.18}$$

Where $v_r$ is the r-component of the velocity and $v_\theta$ is the $\theta$-component of the velocity.

However the transport equations must be solved in both the r and $\theta$ directions and as such one possible way to approximate its solution is by the creeping flow assumption, with slight modification in the radial velocity due to natural swelling of the polymers. Other types of assumptions could have also been use such as the couette´s flow for example however following the recommendations in the literature this was the method that was adopted [60] [59].

$$v_r = \left[1 - 1,5\left(\frac{r}{S}\right) + 0,5\left(\frac{r}{S}\right)^3\right] cos\theta + \frac{v_{sp}}{\left(\frac{r}{S}\right)^2} \tag{4.19}$$

$$v_\theta = \left[1-,75\left(\frac{r}{S}\right) - 0,25\left(\frac{r}{S}\right)\right] sin\theta \tag{4.20}$$

where $v_{sp}$ is the velocity of the gel–solvent interface and S is the position of the interface

That being said the modeling parameters for this approach consist in the difusivity of the polymer, the velocity of the gel-solvent interface ($v_{sp}$ and the particle radius ($r_0$) [58].

### 4.2.3 Parameter Estimation and Evaluation

For this procedure, a similar approach to the RTD fitting was adopted. For both dissolution models the parameters associated with these equations are estimated through the minimization of the residual sum of squares of the experimentally observed values in

accordance to each respective model parameter– SSp

$$SSp = min_X \sum_i \left(C\left(X, t_i\right) - C_i\right)^2 \tag{4.21}$$

where $C(X, t_i)$ is the estimated concentration,$t_i$ and $C_i$ represent the $i^{th}$ points from the experimentally collected time and concentration datasets, and X is the parameter set for the models: $X = [D_s; r0]$ for the Vrentas and Vrentas rubbery approach, $X = [D_s; k; r0]$ for the Vrentas and Vrentas glassy approach and $X = [D_p; v_{sp}; r0]$ for the Devota *et al* (2014) model [60] [59].

# 5

# Results and Discussion

## Contents


5.1 Experimental: PAT results and observations . . . . . 44

5.2 Residence Time distributions . . . . . 44

5.3 Modeling of Polymer dissolution . . . . . 60

## 5.1 Experimental: PAT results and observations

In this section it is described the results that were obtained from the dissolution tests from the available PAT tools (turbidimeter, viscometer and refractometer) as well as some experimental observations and conclusions regarding this mode of operation.

Table 5.1 shows an overview of the results obtained for each system. In green we have the systems whose target concentrations were achieved and whose overall dissolution process went smoothly. On the other hand, in yellow we present the systems whose experiments were hindered due to accumulation arising from difficult process conditions,constraints even due to natural interactions between the polymer:solvent pairing.

**Table 5.1:** Overview of the result Dissolution trials/PoC for each Polymer:Solvent system - Average dissolution times

| **Solvent System** | **Polymer** | | | |
|---|---|---|---|---|
| | $P_1$ | $P_2$ | $P_3$ | $P_4$ |
| **Dichloromethane:Methanol (80:20)** | **Dissolved (6 min)** | **Dissolved (3 min)** | | |
| **Methanol** | **Accumulation (7 min)** | **Acumulation (6 min)** | | |
| **Acetone** | **Dissolved (4 min)** | | **Dissolved (3 min)** | **Dissolved (3 min)** |

Therefore in section A.3 it is then presented a more in-depth showcase of the results in a system by system (polymer:solvent pairings) and trial by trial approach according the methodology that was previously described as well as the optimization procedures to a achieve a complete dissolution.

Nevertheless, it was found that the process used is widely influenced by the polymer:solvent pair, leaving ample room for optimization in order to obtain the full dissolution of the materials in the systems mentioned.

## 5.2 Residence Time distributions

In this section it is described the results and analysis performed concerning the residence time distribution of each system. Therefore as it was stated to use polymers as tracers themselves, we relate to the previous methodology exposed in chapter 4 whereas:

- The ratio of inertial forces to viscous forces that the fluid is subjected to in relation to the internal movement must be constant throughout the dissolution process so that polymer/tracer concentration does not change the hydrodynamic behaviour-constant Reynolds number.

- Any phenomenon occurring in the system should be considered instantaneous as to not change the global process of flowing. Global dissolution time of the polymer should be lower than the experimental obtained mean residence time.

Lastly, it must be said that all the trials were performed with a 30L reactor operating with a 20L solution with a measured flow rate of 2633 L/h.

### 5.2.1 Reynolds Assessment

As it was stated before, the first step for determining if polymers can indeed be used as tracers for RTD experiments is the assessment of the Reynolds number(Re) which can be determined using the following expression:

$$Re = \frac{\rho_s \cdot v \cdot d_c}{\mu} \tag{5.1}$$

Where $\rho_s$ is the apparent density of the polymer solution, $v$ and $d_c$ are respectively the velocity of the fluid, and the characteristic diameter of the reactor and $\mu$, is the apparent viscosity of the system.

Nevertheless since we are using the data obtained in section 5.1 it is important to reassert the systems and corresponding trials that will be subjected to this analysis as well as each of their conditions. Table 5.2 shows an overview of all the experiments performed as well as some of their key process variables.

**Table 5.2:** Overview of the trials analyses for experimental determination of RTDs

| **Trials** | **Polymer** | **Solvent** | **Initial Temperature (ºC)** | **Liquid Flowrate at solids addition** $(m^3/s)$ |
|---|---|---|---|---|
| #1 | $P_1$ | DCM:MeOH(80:20) | 19.7 | 1.2E-03 |
| #2 | | | 4.5 | 1.2E-03 |
| #3 | | | 5.2 | 1.2E-03 |
| #5 | | MeOH | 13.2 | 1.3E-03 |
| #7 | | | 10.5 | 1.3E-03 |
| #8 | | Acetone | 14.5 | 1.8E-03 |
| #9 | $P_2$ | DCM:MeOH(80:20) | 10.1 | 1.8E-03 |
| #10 | | MeOH | 9.0 | 1.8E-03 |
| #11 | | | 11.5 | 1.8E-03 |
| #12 | $P_3$ | Acetone | 9.4 | 1.8E-03 |
| #13 | | | 8.3 | 1.8E-03 |

As such, with an internal characteristic diameter for the reactor of $d_c = 0.4cm$ the assessment of the hydrodynamics of each system was performed for each of these trials according to equation 5.1, while also simultaneously accounting for the changes in the

solvent flow rate during and after the incorporation of the solids. The results of this assessment as well as the upper and lower limits of acceptance for the variation of the Reynolds number (10% of $Re_0$) results are presented trough the next sections in table 5.3 as well as figures 5.1 to 5.5.

| **Trials** | **Mean Reynolds number ($\bar{Re}$)** | $Re_0$ | **Upper Limit** | **Lower limit** |
|---|---|---|---|---|
| #1 | 135 | 154 | 185 | 120 |
| #2 | 84 | 81 | 89 | 73 |
| #3 | 80 | 83 | 91 | 75 |
| #5 | 41 | 44 | 38 | 48 |
| #7 | 66 | 69 | 62 | 76 |
| #8 | 630 | 660 | 700 | 620 |
| #9 | 24 | 25 | 22 | 27 |
| #10 | 10 | 53 | 58 | 47 |
| #11 | 7 | 32 | 35 | 31 |
| #12 | 1005 | 1007 | 1100 | 900 |
| #13 | 817 | 810 | 890 | 730 |

**Table 5.3:** Upper and Lower limits for the Reynolds number of each trial.** Trial marked red are trials whose variation far exceed the upper and lower limits throughout this evaluation

From the analysis of the results in table 5.3, almost all trials fulfill the constant Reynolds number condition aside from trial #10 and #11 (marked red). One possible explanation for this result lies in the polymer-solvent interactions. In this case considering that we are studying a polymer known for its high viscosity $P_2$ in a medium that its not entirely favourable, although possible, for its dispersion and dissolution, and considering the extremely laminar behaviour such limits of variation can drastically change the hydrodynamic behaviour of the reactor.Additionally it is presented in the next sections a more detailed explanation as a visual reference for the changes in the inertial forces during the RTD experiments.

- **$P_1$ systems**

As it can be seen from figure 5.1 and table 5.3 the ratio of inertial forces to viscous forces that the fluid is subjected $T_0$ is constant throughout the dissolution process for any of these experiments meaning that for these systems at these operating conditions any hydrodynamics changes that arise from the polymer introduction are negligible and the first condition for RTD determination is fulfilled. Additionally, in figure 5.1 (a) although the system does not change the behaviour of the reactor the subtle impact of the initial and process temperature on the viscosity and on the hydrodynamic behaviour of the reactor can also be observed. This is translated in higher values of the Reynolds number that come from lower viscosities for trial #1 which possesses an initial temperature

($T_0 = 19.5°C$) significantly higher that trial #2 and #3 ($T_0 = 4.5$ and $5.2°C$ respectively). In figure 5.1 (b) the ratio of inertial forces to viscous forces is also constant within the accepted range, however here the effect of the increase in the rotation of the disperser and consequently on the recirculating flow rate of the system is also present, higher flow rates / rotor speeds increase the turbulence of the system raising its Reynolds number as it can be observed and possible shortening the residence time distribution of the system. Lastly, in figure 5.1 (c) the same behaviour present in the other trials is also observed, nevertheless the natural viscosity of acetone increases the turbulence as expected. Overall, the hydrodynamic behaviour of the system is extremely dependent on the polymer:solvent pairing as expected and as such this trial by trial analysis is required.

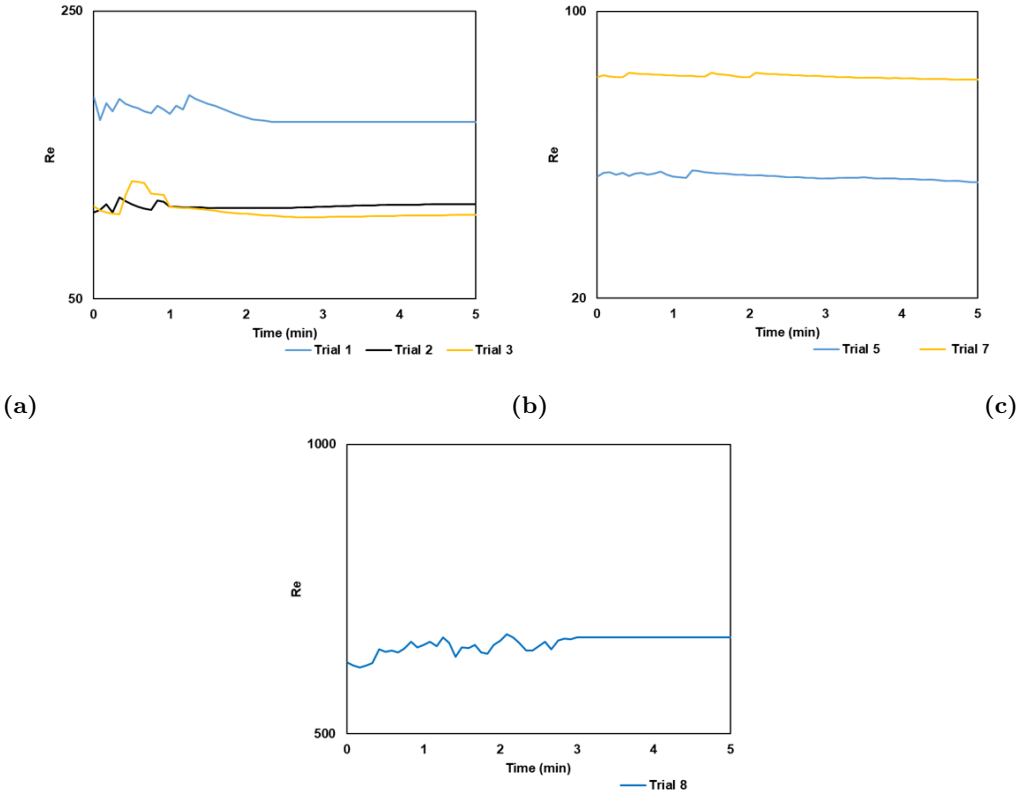


**Figure 5.1:** Reynolds assessment over the solids dissolution time for $P_1$ systems, trials #1; #2,#3; #5; #7 and #8: (a) Reynolds assessment for $P_1$ in 80:20 %w/w of DCM and Methanol (b) Reynolds assessment for $P_1$ in Methanol (c) Reynolds assessment for $P_1$ in Acetone

- **$P_2$ systems**

In trials using $P_2$ due to the natural higher viscosity of the tracer/polymer it is observed a lower value of Reynolds number which is agreement with a more laminar flow present in the reactor. In figure 5.2 (a) trial #9 $P_2$ in DCM:MeOH(80:20) the same behaviour present

in the other trials is observed. The value are within the expected range predicted fulfilling the first condition RTD determination. Nevertheless, in figure 5.2 (b) for systems with $P_2$ and Methanol, it can be seen during the dissolution process that there is a significant variation of the Reynolds number hinting to the possibility that the dissolution cannot be considered instantaneous during the process and the polymer in these systems should not be used as a tracer for the determination of RTDs as the hydrodynamic behaviour of the system varies within the time-frame of the experiment behold the limit values published in the literature.

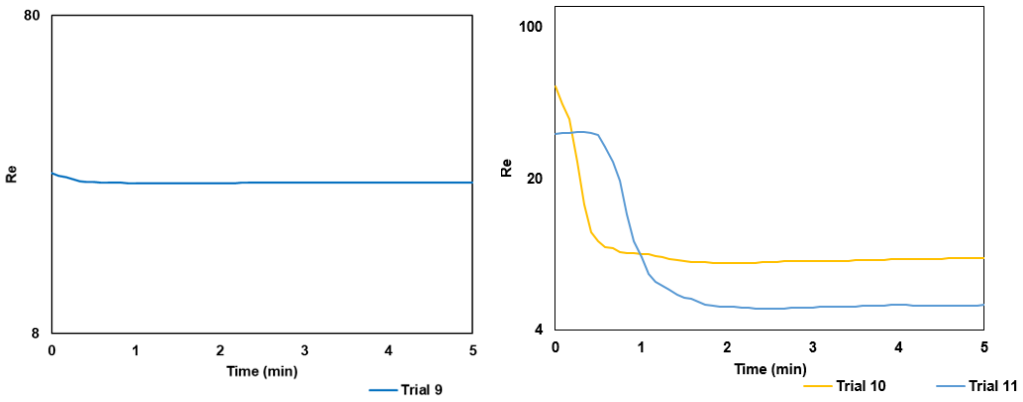


**(a)** **(b)**

**Figure 5.2:** Reynolds assessment over the solids dissolution time for $P_2$ systems, trial #9; #10 and #11: (a) Reynolds assessment for $P_2$ in 80:20 %w/w of DCM and Methanol (b) Reynolds assessment for $P_2$ in Methanol

- **$P_3$ systems**

For trials with $P_3$ due to the low viscosity of the tracer/polymer as well as the low viscosity of acetone these trials serve a benchmark and control in order to assess the other results. There according to the literature as expected the polymer solvent mixture presents very constant ratios of inertial to viscous forces as well as significant turbulence. Additionally, although not high enough to cause troubles it is observed that a small increase in the concentration of the tracer (trial # 13- 10% w/w $P_3$ trial #12 - 8% $P_3$) lowers the turbulence of the system as expected. Overall, in addition to trials #10 and #11, all other systems fulfill the first requirements for RTD determination nevertheless, the mean residence time must also be check to reach definite conclusions.

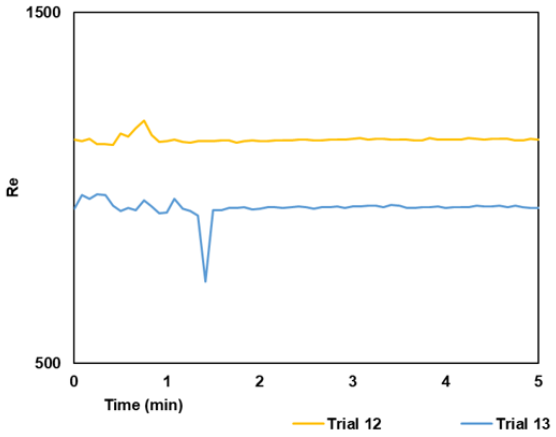


**Figure 5.3:** Reynolds assessment over the solids dissolution time for $P_3$ systems, trial #12; and #13

### 5.2.2 Experimental RTD and Mean residence time

To determine if the polymer dissolution bears any impact in RTD determination (second constraint) it is necessary to preemptively determine the experimental RTD for the each system and calculate and compare its mean residence time to the dissolution times obtained. Again, the determination of the experimental residence time distributions was performed according to the methodology described in chapter 4 where a step like addition of tracer was employed according to the nature of the system and experiments.

The following results have been obtained:

- **$P_1$ in DCM:MeOH(80:20- trials #1; #2 and #3)**

| Trial | Dissolution Time (min) PAT and Visual confirmation | Mean residence time $\bar{\tau}$ (min) | Variance $\sigma^2$ |
|---|---|---|---|
| #1 | 4.0 | 6.8 | 5.3 |
| #2 | 5.0 | 8.3 | 2.2 |
| #3 | 5.0 | 8.1 | 1.9 |

**Table 5.4:** Mean residence times for $P_1$ in DCM:MeOH(80:20) systems for different trials under different conditions. Trial #1 $T_0 = 19,5^{\circ C}$ and 5125 rpm during solids incorporation. Trials #2 and #3 $T_0 = 5.2^{\circ C}$ and $4.5^{\circ C}$ respectively

By analysing table 5.4 it can be seen that as expected the values are similar between all three trials, nevertheless, small changes do exist which can be easily explained by the differences in the initial temperature of each experiment. In trial #1 we have a lower mean residence time than trials #2 and #3 specifically due to this difference. Therefore, by performing the experiment at a higher initial temperature the solution will naturally exhibit a lower viscosity that in turn will facilitate its flow and decrease the solution´s mean residence time in the reactor. Additionally, using the properties of the variance of

experimentally determined RTDs they can provide some insight into what kind of ideal model is better fitted for each system as well as any performance problems of the reactor.Thus, in the most basic sense it is expected that systems whose behavior is similar to a plug flow present lower values of variance (as the RTD are narrower) and systems similar to an ideal mixture that can be modelled by CSTRs (continuous stirred tank reactors) present higher values. Also, the existence of consistency problems such as dead volume, by-pass or preferential paths and even internal recirculation can also be reproduced into an increase of the variance of he RTD. Nevertheless, despite all this, this parameter alone only provides clues to these questions and further analysis for each one is required to draw definite conclusions as it will be seen in later sections.

Lastly and most important from the results obtained it is seen that all these experiments follow both the conditions previously described, *Re constant* and Dissolution time $< \bar{\tau}$ meaning that polymers can indeed be considered tracers for this set-up.

To complement the previous analysis in figure 5.4 it is presented the experimental RTD for each trial.

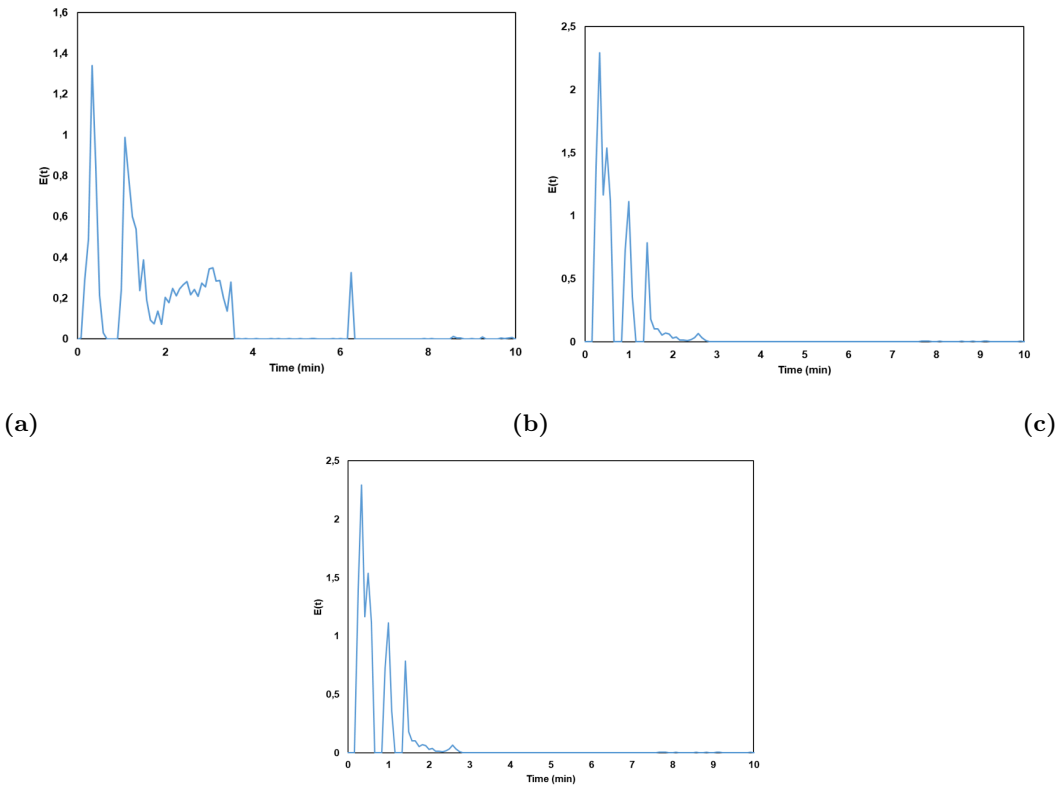


**Figure 5.4:** Experimental Residence Time distributions for each system determination by step administration of tracer: (a)Trial #1 (b) Trial #2 (c) Trial #3

Thus, from the overall shape of the RTD it can be considered the idea of some op-

erational problems within the reactor either due to internal recirculation of the fluid, adsorption of the tracer on the walls or preferential paths. Therefore, according to the literature not only does this shape of RTD mimics traditional systems with internal recirculation but also low variance values ($\sigma^2 = 5$ and $\sigma^2 = 2$) support this possibility, hinting to a probable model of plug flow with internal recirculation. Furthermore, it can be seen that for trials 2 and 3 the residence time distributions are extremely similar showing that these experiments were performed correctly with good results and supporting the reproductibility of the the set-up since the trials were performed under the same conditions.

- **$P_1$ in MeOH- trials #5 and #7**

| **Trial** | **Dissolution Time (min) PAT and Visual confirmation** | **Mean residence time $\bar{\tau}$ (min)** | **Variance $\sigma^2$** |
|---|---|---|---|
| #5 | 10.2 | 12.1 | 7.5 |
| #7 | 7.0 | 9.4 | 5.7 |

**Table 5.5:** Mean residence times for $P_1$ in MeOH under different recirculating flowrates, Trial #5 5125 rpm and Trial #7 7295 rpm

In these systems we can observe that the results in table 5.5 are relatively similar and in accordance to all the established conditions ($Re = constant$ and Dissolution time $< \bar{\tau}$) but still different enough to accommodate the discrepancies in the operating conditions of each trial. Thus, in trial #5 it is observed a slightly higher mean residence time as a result of the lower operating flow rate that was used when compared to trial #7 (2633 L/h and 4000L/h respectively). Lastly, from the values obtained all these experiments follow both the conditions previously described, meaning that the dissolving polymer can be used as a tracer option in the determination of experimental RTDs.

Furthermore, to complement the previous analysis in figure 5.5 it is presented the experimental RTD for each trial.

Again from the initial analysis of the results, it is observed a much wider distribution, supported by the overall mean residence time and variance values when compared to trials using $P_1$ in DCM:MeOH(80:20) (table 5.5) and figure 5.4). This is as expected as we are testing entirely different fluids and systems with different properties and behaviours. In addition the natural high viscosity of $P_1$ in methanol solutions causes the system to behave in a more laminar manor changing and shifting the shape of the RTD, therefore this by itself suggests that a more similar to a single or a battery of CSTRs is more suitable to describe the behaviour, nevertheless additional studies for these systems will be presented in the forthcoming sections.

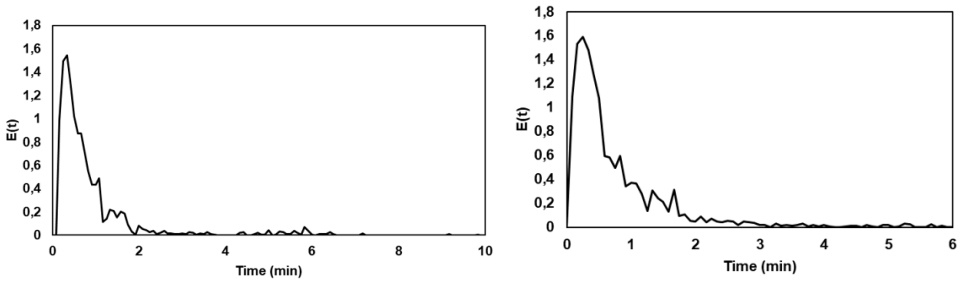


**(a)** **(b)**

**Figure 5.5:** Experimental Residence Time distributions for each system determination by step administration of tracer: (a)Trial #5 (b) Trial #7

- $P_1$ **in Acetone- trial #8**

| Trial | Dissolution time- PAT and visual confirmation (min) | Mean residence time- (min) | Variance $\sigma^2$ |
|---|---|---|---|
| #8 | 4.0 | 6.8 | 3.1 |

**Table 5.6:** Mean residence time for $P_1$ in Acetone systems- trial #8

For $P_1$ in acetone, it is observed that both $Re = constant$ and Dissolution time $< \bar{\tau}$ satisfying the conditions established for the proper analysis of RTDs, however by comparing the values of both $\bar{\tau}$ and $\sigma^2$ to other trials using the same polymer it is observed that these values are much smaller then their counterparts.

Again in figure 5.6 lies the experimentally obtained RTD.

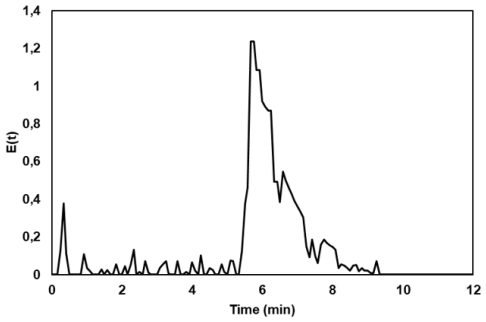


**Figure 5.6:** Experimental Residence Time distributions for each system determination by step administration of tracer: Trial #8

- $P_2$ **in DCM:MeOH(80:20)-trial#9**

Moving on to $P_2$ systems, when using DCM:MeOH(80:20) as a solvent the same conditions previously established still verify ($Re = constant$ and Dissolution time $< \bar{\tau}$) meaning the polymer can be used as a tracer for the determination of RTDs.

| Trial | Dissolution time- PAT and visual confirmation (min) | Mean residence time- (min) | Variance- |
|---|---|---|---|
| #9 | 7.0 | 7.8 | 3.1 |

**Table 5.7:** Mean residence time for $P_2$ in DCM:MeOH(80:20) systems- trial #9

Figure 5.7 shows the experimentally obtained RTD.

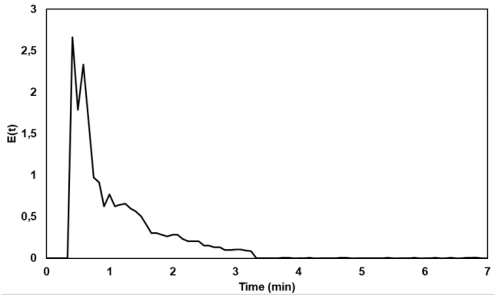


**Figure 5.7:** Experimental Residence Time distributions for each system; determination by step administration of tracer: Trial #9

- **$P_3$ in Acetone- trials #12 and #13**

| Trial | Dissolution Time (min) PAT and Visual confirmation | Mean residence time (min) | Variance |
|---|---|---|---|
| #12 | 2 | 3.6 | 0.4 |
| #13 | 2 | 3.9 | 0.7 |

**Table 5.8:** Mean residence times for $P_3$ in Acetone under different conditions. Trial #12-$C_{tracer} = 8\%w/w$. Trials #13- $C_{tracer} = 10\%w/w$

For systems using $P_3$ and acetone the conditions are also met, however here we observe the highest peaks for the residence time distributions and the narrowest distributions; lower variance. This result was only as expected because as it was said before these trials serve as a control group to the overall analysis due to the low viscosity ($\mu < 1$) and high turbulence of the system ($Re > 10000$) which not only renders all possible changes of the hydrodynamic behaviour of the system during tracer addition null but also disregards other possible facts that come with the dissolution of the polymer as it is nearly instantaneous (below 2 min). Additionally, from a preliminary standpoint it can be said that this characteristic RTD of extremely high peak and very narrow distributions is congruent with an ideal plug flow behaviour where there is only one residence time whose peak intensity reaches to infinity.

Figure 5.8 shows the experimentally obtained RTDs.

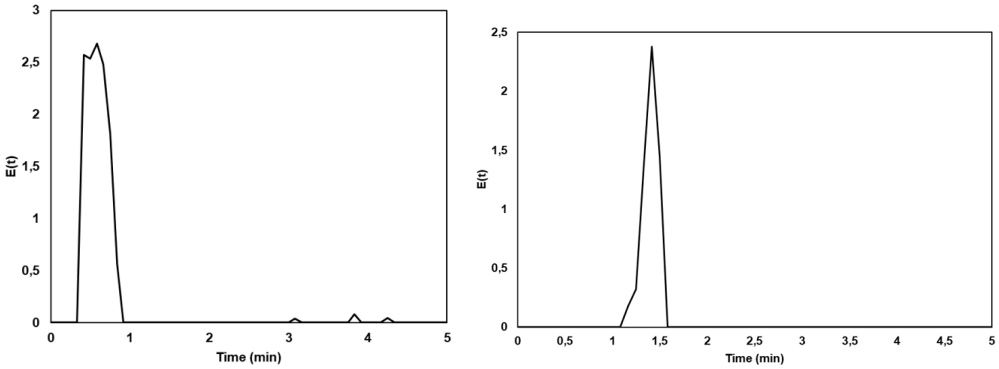


**(a)** **(b)**

**Figure 5.8:** Experimental Residence Time distributions for each system determination by step administration of tracer: (a)Trial #12 (b) Trial #13

### 5.2.3 Consistency Tests

When experimentally determining residence time distributions it is always important to measure and evaluate all changes in the flow patterns of a rector. The most important reasons for the changes in the flow pattern can be the existence of dead volume due to the formation of poorly agitated areas causing fluid motion to stagnate, as well as the existence of preferential paths, which entails that some of the fluid mixture flows directly towards the exit of the reactor. These problems can easily be detected with two simple consistency tests.

- The first test is the comparison between the inlet tracer quantity and the total quantity that can be determined at the outlet of the reactor:

$$\frac{N_s(t)}{Q} = C_0 \int_0^t E(t')dt' \tag{5.2}$$

- The second test consists in comparing the mean experimental residence time with the residence time obtained from the known volume and flowrate of the reactor,therefore:

$$\bar{\tau} = \frac{V_{efective}}{Q_{efective}} = \frac{V - V_{dead}}{Q_e} = \frac{V_{reactor}}{Q} \tag{5.3}$$

$$\frac{N_s}{N_e} = \frac{Q_e}{Q} \tag{5.4}$$

Thus, under ideal operating conditions the quantity of tracer detected in the reactor outlet should be equal to inlet tracer quantity ($N_s = N_e$) and the experimental residence

time should also be similar to the characteristic residence time of the reactor($\tau_{theoretical} = 0.46\ min$).

Therefore in table lies 5.9 the comparison of the inlet and outlet tracer quantities as well as the mean residence times of all systems that were studied. All tracer inlet quantities can be explained throughout the process depicted in section 5.1.

| **Trial** | **Tracer in - Ne (Kg)** | **Tracer Out - Ns (Kg)** | **Mean residence time $\bar{\tau}$ (min)** |
|---|---|---|---|
| #1 | 1.37 | 1.12 | 6.8 |
| #2 | 1.54 | 1.38 | 8.3 |
| #3 | 1.58 | 1.33 | 8.1 |
| #5 | 1.37 | 0.96 | 12.1 |
| #7 | 1.37 | 1.05 | 9.4 |
| #8 | 1.37 | 1.28 | 6.8 |
| #9 | 1.37 | 1.23 | 7.8 |
| #12 | 1.37 | 1.35 | 3.6 |
| #13 | 1.88 | 1.79 | 3.9 |

**Table 5.9:** Comparison between the inlet and outlet tracer amount for the consistency tests

From the results presented in table 5.9, it can be seen that there is a lack of consistency of the results, meaning that the flow pattern of each system deviates from an ideal behaviour. Possible causes for this issue can come not only from the existence of dead volume or preferential paths but also due to the adsorption of the tracer to the reactor walls or to the probe used for determining its concentration or the existence of an internal recirculating flow rate. The existence of theses problems for operating flow pattern are supported by the RTD which translate these results. For example, in trial 1 through 3 it can be seen the a typical case of internal recirculation as the RTD repeats itself trough the RTD towards higher residence times with can be explained either by small differences in the effective flow rate measured flow rate or the the adsorption of tracer to the walls of the reactor or the probe used to determine its outlet concentration.

Nevertheless, the most relevant problems for the operating conditions are the existence of dead volume and preferential paths which in the context of the proof of concept can firstly mean that there are poorly agitated areas within the reactor that can hinder the dissolution process but also that since there was no mechanical agitation inside the reactor (all the agitation and turbulence required for the system came from the disperser that was used as a pump) these are the worst case scenarios with significant room for improvement. Lastly, table 5.10 shows the quantification of the problems depicted before. These values could allow for the elaboration of RTD models that account for these problems, however due to insufficient time for this works this was not possible.

| Trial | Dead volume (L) | By pass flowrate (L/h) |
|---|---|---|
| #1 | 2.6 | 333 |
| #2 | 2.2 | 354 |
| #3 | 2.3 | 375 |
| #5 | 3.5 | 551 |
| #7 | 3.1 | 519 |
| #8 | 1.9 | 237 |
| #9 | 2.7 | 288 |
| #12 | 1.7 | 112 |
| #13 | 1.3 | 134 |

**Table 5.10:** Quantification of the bypass and dead volume when compared to existing flow rate and rector volume

Overall, the presence of some dead volume can be observed where the fluid motion is stagnant as well as some preferential paths, nevertheless these operating problems are no greater than 10% of the original process conditions which means that there is still room for improvement as the experiments were performed under a worst case scenario assumption. Additionally other reasons for the lack of consistency in the results point towards the adsorption of the tracer to the reactor walls due to the natural stickiness of the polymers despite being kept to a minimum.

### 5.2.4 RTD modeling based on ideal reactors

In this section we present some of modelling results that were performed to analyse the real system behavior. The experimental results were compared to ideal models such as CSTR, plug flow behaviour or even laminar flow for simplicity, however other more complex models that account for the the existence of dead volume, preferential paths and internal recirculation could have also been employed but due to some time constraints and schedules associated with the project these were not used. Convolutions between the ideal models were also tested.

- **$P_1$ in DCM:MeOH(80:20- trials #1; #2 and #3)**

As it was said before, the experimental residence time distribution for this system follows a typical plug flow behaviour, characterized by a sharp surge in the RTD, however as stated previously the presence of internal recirculation is evident as there are multiple other spikes with decreasing intensity that fall under a plug flow behaviour as well.This behaviour accompanied by the some existing results in the literature point towards the trend. The RTD obtained were already presented in figure 5.4(a)

- **$P_1$ in MeOH- trials #5; #7**

For $P_1$ in pure methanol, the modeling results are depicted in figure 5.9 to 5.12. Several ideal models were tested: CSTR, plug flow, laminar flow and convolutions between them either in parallel or in series. The modeling approach was previously introduced in chapter 4

From the analysis of figure 5.9 it can be seen that the most suitable ideal model for the representation of this system is a battery of 2 CSTR in series with identical volume as it can be observed from not only the matching RTDs but also due to the accurate outlet concentration outlet prediction. Additionally both trials #5 and#7 do not have the same operating conditions, in comparison trial #7 was performed with a slightly higher recirculating flow rate, nevertheless both trials successfully predict the same modeling representation, validating the reproductibility of the method used and process.

Lastly, it is expected that systems with $P_1$ in methanol whose inherent viscosity is generally higher than other systems with different solvents like acetone for example, tend to be represented by ideal models which typically have higher mean residence times such as CSTRs.This hypothesis as it can be seen is demonstrated in figure 5.9. On the other hand, acetone systems that typically have a low viscosity are expected to have more suitable representations using models that express this behavior such as plug flow.

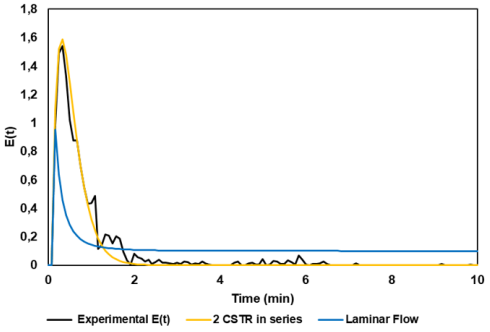


**Figure 5.9:** Trial #5 Modeling Response

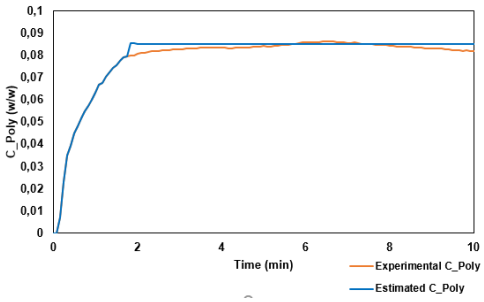


**Figure 5.10:** Trial #5 Concentration Prediction vs Experimental

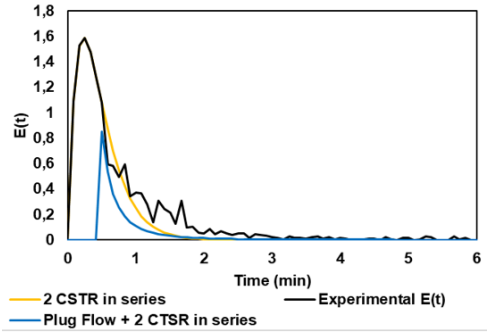


**Figure 5.11:** Trial#7 Modeling Response

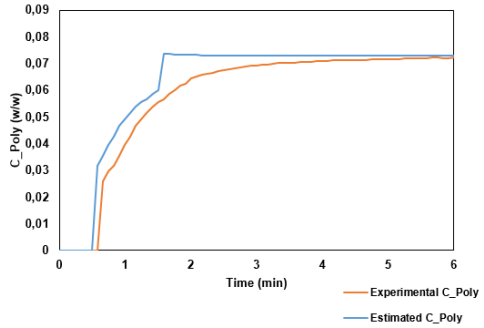


**Figure 5.12:** Trial #7 Concentration Prediction vs Experimental

- **$P_1$ in Acetone- trials #8**

For $P_1$ in pure acetone, the modeling results are depicted in figure 5.13. The same approach introduced in chapter 4.2.1 was used. As it can be seen the model that best fits the experimental data is a plug flow in series with a battery of 2 CSTR also in series.

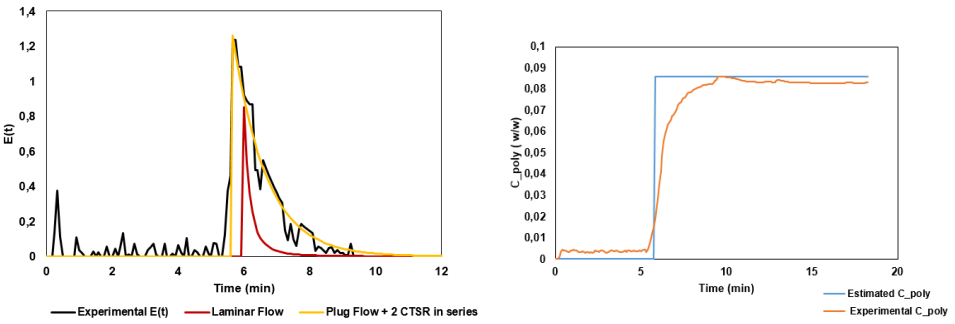


**(a)** **(b)**

**Figure 5.13:** Modeling of the experimental residence time distributions for trial #8 and its corresponding concentration prediction

- **$P_2$ in DCM:MeOH(80:20)- trials #9**

For $P_2$ in dichloromethane and methanol mixtures (80:20 %w/w), the modeling results are depicted in figure 5.14. In this instance despite trial 9 ($P_2$ in DCM:MeOH (80:20)) being an entirely different system than trial 8 ($P_1$ in acetone) it can be seen the model that best fits the experimental data is also a plug flow in series with a battery of 2 CSTR also in series. One possible reason for this behaviour tend to be due to the viscosity of both systems, since their are relatively similar it expected that they have the fluids when under the same conditions have the same behaviour and can be modeled by the same approach.

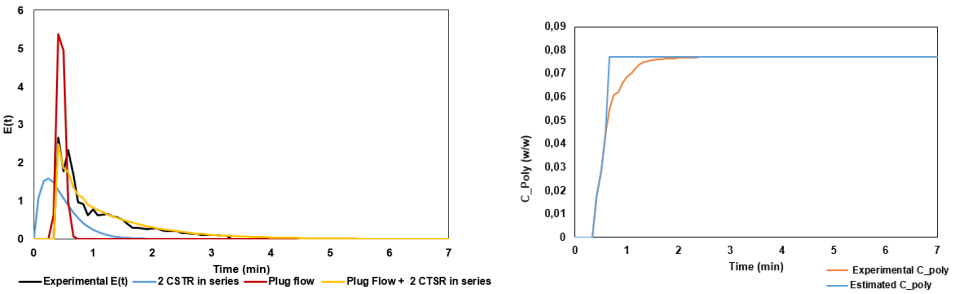


**(a)** **(b)**

**Figure 5.14:** Experimental Residence Time distributions for each system determination by step administration of tracer: (a)Trial #5 (b) Trial #7

- **$P_3$ in Acetone- trials #12 and #13**

Lastly for systems with $P_2$ and acetone it can be seen that their fit is a classical plug flow, which was expected due to the inherent low viscosity.

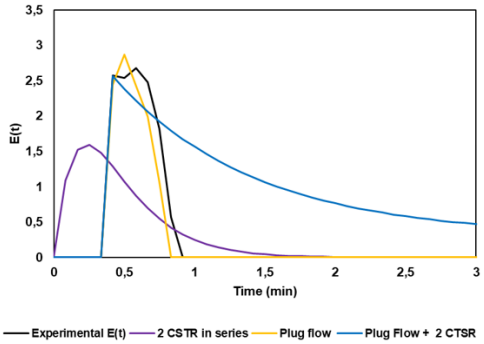


**Figure 5.15:** Trial #12 Modeling response

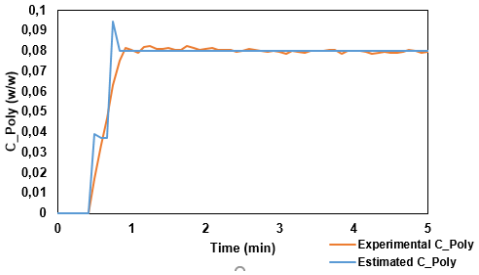


**Figure 5.16:** Trial #12 Concentration prediction vs experimental

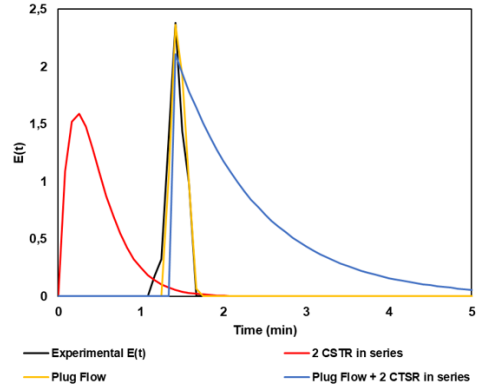


**Figure 5.17:** Trial#13 Modeling response

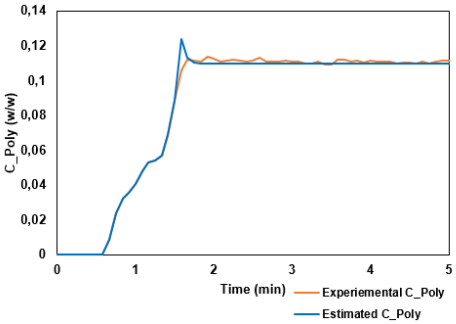


**Figure 5.18:** Trial #13 Concentration Prediction vs Experimental

## 5.3 Modeling of Polymer dissolution

Regarding polymer dissolution models it was also studied the possibility of predicting not only the dissolution time of a polymeric powder in a given system but also its concentration profile during the dissolution process. Therefore, the two models described in chapter 4 were utilized according to the methodology explained previously, Vrentas and Vrentas (1998) with both glassy and rubbery dissolution approaches and the moving stream of solvent dissolution model from Devota *et al* (2014). Nonetheless, this study was only performed to two existing systems due to time constraints and using the same nomenclature throughout this document the trials utilized were #8 , #12 and #13 being respectively $P_1$ in Acetone and $P_3$ also in acetone at a target concentration of 8 and 10% w/w. As such the results are presented in figure 5.19.

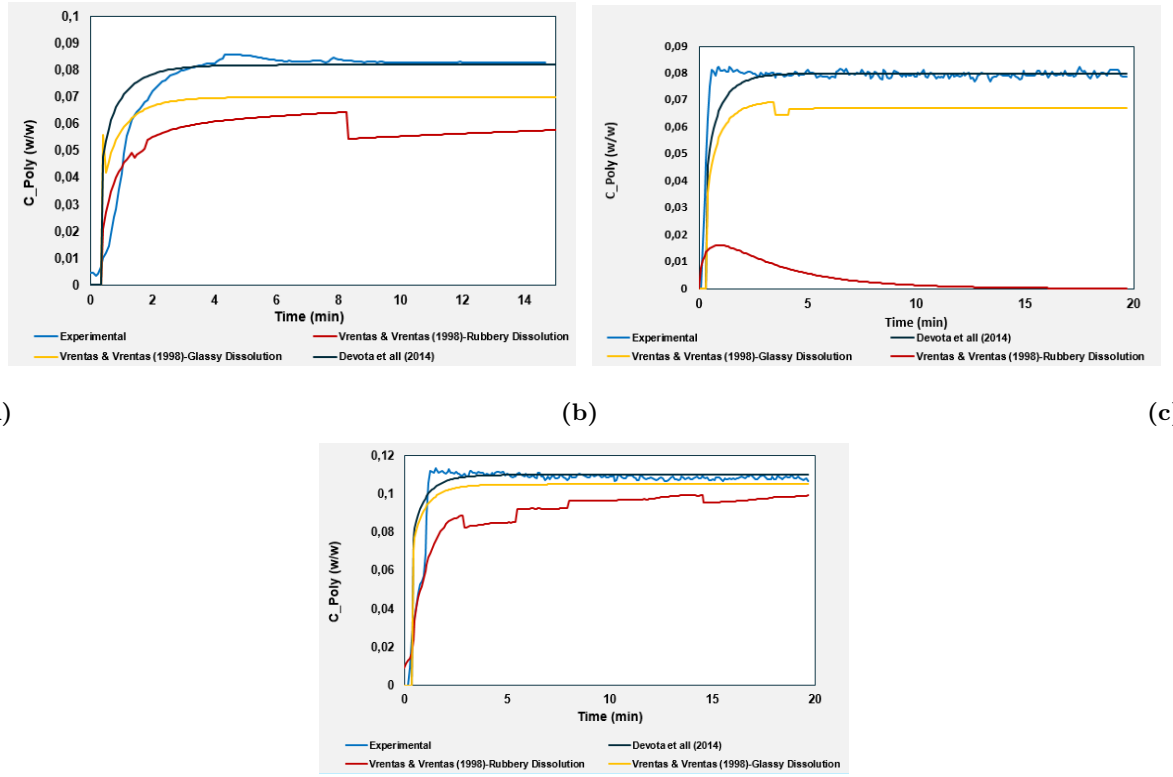


**Figure 5.19:** Polymer dissolution model concentration profiles and its comparison to the experimental data: (a)-Trial #8-$P_1$ in Acetone at 8% w/w (b)-Trial #12 $P_3$ in Acetone at 8%w/w (c)-Trial #13 $P_3$ in Acetone at 10% w/w

For the Vrentas and Vrentas (1998) rubbery dissolution we have the following results, as it can be seen this model falls extremely short for all the experimental data. One possible reason for this behavior falls back on the model characteristics and its assumptions on a particle level. Thus, since the model assumes that the transition from the glassy state to

the rubbery state is instantaneous, meaning that the swelling of polymer particle during solvent penetration is negligible which the limiting step in the dissolution process is the polymer diffusion to the bulk solution which for most polymer:solvent pairing is not the case. This approach coupled with an assumption that the diffusivity coefficient of the polymer is constant trough the dissolution process validate the differences between the experimental data and the results obtained by the model. Nevertheless,it can also be seen that for systems using $P_3$ regardless of the quantity of polymer to be dissolved the differences between the experimental values and the values predicted are significantly lower than in systems using $P_1$. Therefore, this hints to the possibility that solvent penetration in $P_3$ and acetone systems is not as relevant, since the polymer solvent interactions allow for a swift and rapid penetration in the polymer particle that is translated in lower dissolution times.

Lastly, in table 5.11 we present the results for the modeling parameters of this approach and its comparison the literature values and experimental data.

| **Trial** | **Diffusion Coefficients**** ($cm^2/s$) | **Diffusion Coefficient Model** ($cm^2/s$) | **Dissolution time (min)- Model** | **Dissolution time (min) Experimental** | **Particle radius (nm)** |
|---|---|---|---|---|---|
| 8 | 3.42E-11–6.18E-10 | 2.14E-9 | 10 | 4 | 130 |
| 12 | 7.45E-7–8.69E-8 | 9.31E-5 | NA | 2 | 300 |
| 13 | | 3.57E-6 | 12 | 3 | |

**Table 5.11:** Vrentas and Vrentas Rubbery dissolution model parameters.** Values obtained from literature [7] [8]

An additional approach of the Vrentas and Vrentas model (1998) was also studied, where it is assumed that the polymer is in a glassy state as the dissolution commences. As such, contrary to the previous approach this approach takes into account the changes in the diffusivity coefficient of the system introducing a another modeling parameter( $k$, where $\frac{D}{D_s} = exp\,(k \cdot C_p)$) that symbolizes the resistance of the polymer chain to achieve the adequate configuration in the glassy state before it disengages and dissolves in the bulk of the solution. Thus, as expected this approach usually fares much better for systems whose polymer solvent interactions are not optimal as it is the case for $P_1$ in acetone when compared to $P_3$ in the same solvent. Moreover, this response is corroborated by the experimental dissolution times between these two systems as $P_1$ trials have a significantly higher dissolution time due to its interaction with acetone. Nevertheless using this approach the model still falls short from the expected values, however it represents a much accurate representation of the system.

Lastly it was decided to use the, Devota *et al* (2014) model which takes into account a moving stream of solvent causing the concentration field during the dissolution process to not be uniform whilst adding an additional parameter to the modeling procedure. As

| Trial | Diffusion Coefficient** ($cm^2/s$) | Diffusion Coefficient Model ($cm^2/s$) | Dissolution time (min)- Model | Dissolution time (min) Experimental | Particle radius (nm) | $k$ |
|---|---|---|---|---|---|---|
| 8 | 3.42E-11–6.18E-10 | 1.78E-11 | 10 | 4 | 130 | 0.79 |
| 12 | 7.45E-7–8.69E-8 | 6.33E-7 | NA | 2 | 300 | 1.35 |
| 13 | | 1.59E-7 | 12 | 3 | | 1.37 |

**Table 5.12:** Vrentas and Vrentas Glassy dissolution model parameters.** Values obtained from literature [7] [8]

it can be seen from figure 5.19, the creeping flow approach presents itself as a suitable solution for the velocity field component of the transport equations of the model. Additionally this also assume that the limiting step of the dissolution process is the diffusion of the disentangled polymer chains to the bulk of the solution, however the additional modeling parameter allows for compensation for the other existing phenomenon contrary to the other models. In table 5.13 we present the results of the model parameter that were obtained and by carefully analysing the results it can be seen the all values are within the expected range of the data obtained from other author who used the same approach.

| Trial | Difusion Coeficient** (cm2/s) | Difusion Coeficient Model (cm2/s) | Dissolution time (min)- Model | Dissolution time (min) Experimental | Particle radius (nm) | $v\_sp(nm/s)$ |
|---|---|---|---|---|---|---|
| 8 | 3.42E-11–6.18E-10 | 4.77E-10 | ∼4 | 4 | 130 | 1.21 |
| 12 | 7.45E-7–8.69E-8 | 9.31E-7 | ∼2 | 2 | 300 | 3.78 |
| 13 | | 2.85E-8 | ∼2 | 3 | | 3.16 |

**Table 5.13:** Devota *et al.* (2014) dissolution model parameters.** Values obtained from literature [7] [8].

Overall, this model is the one that presents better results for both experimental trials and whose modeling parameters that were obtained are relatively accurate when compared to the values presented in the existing literature.

# 6

# Conclusions and Future Work

## Contents

6.1 Conclusions . . . . . 64

6.2 Future Work . . . . . 65

## 6.1 Conclusions

The objective of this dissertation was to evaluate the dissolution end-point of polymers and concentration using certain PAT equipment in order to establish a proof of concept of an experimental set-up for all pharmaceutical process involving polymer dissolution.

Regarding the establishment of the proof of concept, it was found that for all systems and process conditions studied, the dissolution process occurred smoothly as the target concentration was achieved under an average time of up to 10 min. Nevertheless, due to the polymer solvent interactions, systems using $P_1$ in ethanol may require additional optimization as in some cases a thin layer of floating polymer was formed at the surface of the reactor, however with increasing agitation it was observed that it was reduced. Additionally the set-up studied was found to have some reproducibility for systems using $P_1$ in DCM:MeOH (80:20) mixtures. The results produced nearly identical responses for all PAT data and similar dissolution times. Nevertheless, DCM systems were also found to be extremely sensitive to the process temperature due to the inherent heat transfer that arises from the operating recirculating pump.

Regarding material tracking techniques, it was established the idea of using Residence times distributions for such task. Therefore, it was concluded that it is possible to determine RTDs using polymer powders as tracers only if certain conditions were met: constant Reynolds number and a dissolution time that should be lower than the mean residence time of the RTD. As a result, of all systems that were studied, only $P_2$ in methanol was found to not be feasible for such determination due to the high viscosity of the system that caused changes in the hydrodynamic behavior of reactor. Additionally, it was found that virtually all the systems that were studied under these conditions have consistency problems such as dead volume and preferential paths due to the existence of poorly agitated areas. This is due to the designing of the reactor and also because the only mechanical agitation came from the disperser that acted as a recirculating pump.

Also, other causes for the lack of consistency of the results were also found to be present although on a much minor scale as some adsorption of the tracer to wall was confirmed visually. For trials with $P_1$ in DCM:MeOH(80:20) by using model examples in the literature internal recirculating was also found to be present.

The ideal modeling of the RTDs to try to fit the experimental values to the ones obtained through the method that was used, showed that when analyzing the possibility of using polymer powders as tracer the system is extremely dependent on the polymer solvent interactions. In this work, it was also verified that systems whose inherent viscosity is generally lower pointed towards a plug flow pattern, which was the case for $P_3$ systems

in acetone and as the viscosity of the system increased the behavior shifted to something more similar to a CSTR. Lower viscosities tended to provide RTDs that could be explained by intermediate models between the two opposite models such as a plug and a battery of 2 CSTR in series as it was the case for trials 8 and 9. Lastly, the possibility of using polymer dissolution thermodynamic models to predict the end-point of the dissolution and establish the concentration profile were also analyzed. From the results obtained it could be concluded that the models who did not take into account the changes in the polymeric particle from its glassy state to rubbery state due to the solvent penetration, as well the disengagement dynamics of the polymer chain fell short when predicting not only the properties of the system but also the responses of the system as well.

## 6.2 Future Work

In this work it was not possible to really investigate the impact of the CPPs due to the time limitations. Therefore, some intended experiments/tasks are referenced for future work. As such, the next step further after establishing this proof of concept would be to perform the same dissolution studies while including API for the purpose of drug formation whilst simultaneously coupling the existing set-up to another unit, for example such as spray dryers, crystallizer, extruder etc.. and assess if any of the CQAs and CPPs are affected. Moreover, other methodologies relying on theoretical equation could have been used in order to determine the relationship between viscosity, temperature and concentration. The literature is extensive in this area however empirical relationships such the Huggins-Kramer equation or the vant´ off equation for determining the concentration could have been used as well instead of relying in offline measurements and calibrations, unfortunately due to limited time this was not possible

Additionally due to some time restrictions other possible residence time distributions models that are more generalized for non-ideal reactor were not studied. Expanding the analysis of this topic to the Taylor model of axial dispersion or the stochastic model and markov chains could have been extremely beneficial and could have provided some insight into forms of automatic control options as these models are commonly used in conjunction with Model Predictive Control in techniques for tablet selection in the pharmaceutical industry

Furthermore, in the realm of polymer dissolution models due to time constraints it was not possible to use a wider variety of polymers and solvents which could have been extremely beneficial in order to extrapolate more insight into the dynamics of the dissolu-

tion for the existing system. Additionally other solution to the transport equation of the Devota *et al* (2014) model could have been employed, another commonly used solution would the couette´s instead of the creeping flow solution which could have provide even more accurate results and conclusions.

# Bibliography


[1] U. Asmussen F, "Velocity of dissolution of polymers," *Diffusion in polymers Part II. J Polym Sci (3) 16 120-141*, 1962.

[2] M. S. Narasimhan B, "Dissolution of amorphous and semicrystalline polymers: mechanisms and novel applications." *Journal of Polymer science (11)*, 1998.

[3] Ueberreiter, "The solution process," *Diffusion in polymers. New York, NY: AcademicPress*, 1968.

[4] S. Martínez and C. Barrera-Díaz, "Residence time distribution and back-mixing in a tubular electrochemical reactor y. gao et al. / powder technology 228 (2012) 416–423 421 operated with different inlet flow velocities, to remove cr(vi) from wastewater." *Polym Engng Sci*, Chemical Engineering Journal 165 (3) (2010) 776–783.

[5] C. Cooney, "Regulatory and quality considerations for continuous manufacturing," May 2014.

[6] F. Guidelines, "International society for pharmaceutical engineering good automated manufacturing practice (gamp) good practice guides," May 2011.

[7] A. Vanarase, "Real-time monitoring of drug concentration in a continuous powder mixing process using nir spectroscopy," *Chemical Engineering Science, 65(21), 5728–5733.*, 2010.

[8] H. Kaneko, "Development of a new soft sensor method using independent component analysis and partial least squares," *AIChE Journal,55(1), 87–98.*, 2009.

[9] S. Vehring, "Pharmaceutical research, vol. 25, no. 5," May 2008.

[10] M. K. Nasr, M, "Regulatory perspectives on continuous pharmaceutical manufacturing: Moving from theory to practice," *International Symposium on the Continuous Manufacturing of Pharmaceuticals*, 2017, September.

[11] EMA, "European medicines agency guideline on real time release testing," October 2012.

[12] U. department of Health, I. services; Food, and D. Administration, "Quality considerations for continuous manufacturing guidance for industry." February 2019.

[13] FDA, "Process validation: General principles and practices," January, 2011.

[14] A. Singh and Z. Worku, "Oral formulation strategies to improve solubility of poorly water-soluble drugs," *Expert Opin. Drug Deliv. 8*, 2011.

[15] A. Singh and V. G., "Polymeric delivery systems for poorly soluble drugs," *Encyclopedia of Pharmaceutical Science and Technology, fourth ed.Taylor and Francis*, 2013.

[16] N. McCrum, P. Buckley, and C. B. Bucknall, "Principles of polymer engineering," Oxford University Press, Oxford, 1997.

[17] C. Hancock and M. Parks, "What is the true solubility advantage for amorphous pharmaceuticals?" *Pharm. Res. 17*, 2000.

[18] C. Hancock and G. Zografi, "Characteristics and significance of the amorphous state in pharmaceutical systems part ii," *J. Pharm. Sci. 86*, 1997.

[19] G. Zografi, "Characteristics and significance of the amorphous state in pharmaceutical systems," *J. Pharm. Sci. 86*, 1997.

[20] P. M. A. Dokoumetzidis, "A century of dissolution research: from noyes and whitney to the biopharmaceutics classification system," *Int. J. Pharm. 321*, 2006.

[21] C. Hancock and M. Parks, "What is the true solubility advantage for amorphous pharmaceuticals," *Pharm. Res. 17 397–404*, 2000.

[22] G. R. Rodriguez F, Krasicky PD, "Dissolution rate measurements: Solid state." *Polym Engng Sci (35) 23-44*, 1996.

[23] W. Cooper, "Dissolution rates of poly(methyl methacrylate) films in mixed solvents," *Polym Engng Sci (19) 123-134*, 1986.

[24] G. RJ and R. F, "Dissolution rates of polymers and copolymers based on methyl, ethyl, and butyl methacrylate." *Polym Engng Sci*, 1989.

[25] J. P. DW Hess, "Swelling of poly(methyl methacrylate) thin films in low molecular weight alcohols," 1980.

[26] A. G. RS Harland, "Drug–polymer matrix swelling and dissolution." *Polym Engng Sci (21) 452-467*, 1988.

[27] A. Ouano and C. Carothers, "Dissolution dynamics of some polymers: solvent–polymer boundaries," *Polym Engng Sci (20) 99-109*, 1980.

[28] L. H.-J. Reinhardt M, Pfeiffer K, "Polymer dissolution: On the dissolution behavior of copolymers of methyl methacrylate and methacrylic acid," *Journal of Applied Polymer Science (77) 86-120*, 1994.

[29] G. E, O. AC, and J. DE, "Parameters affecting the sensitivity of poly(methyl methacrylate) as a positive lithographic resist," *Polym Engng Sci (17) 7-23*, 1977.

[30] A. Ouano, "Dissolution kinetics of polymers: effect of residual solvent content," *Macromolecular solutions: solvent–property relationships in polymers. New York, NY: Permagon Press;*, 1982.

[31] T. Porfirio and J. Vicente, "Rheological characterization of polymeric solutions used in spray drying process," *European Journal of Pharmaceutical Sciences, Volume 157*, 2020.

[32] D. F. James, "Boger fluids," *Annu. Rev. Fluid Mech. 2009. 41:129–42*, 2009.

[33] L. Campo-Deaño and F. J. Galindo-Rosales, "Flow of low viscosity boger fluids through a microfluidic hyperbolic contraction," *J. Non-Newton fluids Mech.166*, 2010.

[34] N. O. V. Shilapuram, D. Jaya Krishna, "Residence time distribution and flow field study of aero-shielded solar cyclone reactor for emission-free generation of hydrogen." *International Journal of Hydrogen Energy 36 (21) (2011) 13488–13500.*, 2011.

[35] M. Larochette, D. Nasri, and F. Léonardi, "Optimization of the polymer foam process by the residence time distribution approach." *Industrial and Engineering Chemistry Research 48 (10) (2009) 4884–4891*, 2009.

[36] P. Danckwerts, "Continuous flow systems: distribution of residence times." *Chemical Engineering Science 2 (1) (1953) 1–13.*, 1953.

[37] E. Nauman, "Residence time theory." *Industrial and Engineering Chemistry Research 47 (10) (2008) 3752–3766.*, 2008.

[38] A. L. P. Markström, N. Berguerand, "The application of a multistage-bed model for residence-time analysis in chemical-looping combustion of solid fuel," *Chemical Engineering Science 65 (18) (2010) 5055–5066*, 2010.

[39] L. Zhang, "Residence time distribution: an old concept in chemical engineering and a new application in polymer processing." *AICHE Journal 55 (1) (2009) 279–283.*, 2009.

[40] H. Essadki and H. Delmas, "Residence time distribution measurements in an external-loop airlift reactor: study of the hydrodynamics of the liquid circulation induced by the hydrogen bubbles." *Chemical Engineering Science 66 (14) (2011) 3125–3132.*, 2011.

[41] F. M. Y. Gao, M. Ierapetritou, "Periodic section modeling of convective continuous powder mixing." *AIChE Journal 58 (1) (2012) 69–78.*, 2012.

[42] S. M. C.J. Dittrich, "On the residence time distribution in reactors with non-uniform velocity profiles: the horizontal stirred bed reactor for polypropylene production." *Chemical Engineering Science 62 (21) (2007) 5777–5793.*, 2007.

[43] K. J. Lin, B, "A systematic approach for soft sensor development," *Computers chemical engineering, 31(5-6), 419–425.*, 2007.

[44] T. J. Rato and M. S. Reis, "Translation-invariant multiscale energy-based pca for monitoring batch processes in semiconductor manufacturing," *IEEE TRANSACTIONS ON AUTOMATION SCIENCE AND ENGINEERING*, 2017.

[45] I. Jolliffe, "Principal component analysis,," *Sringer*, 2002.

[46] D. B. M. Facco, P., "Moving average pls soft sensor for online product quality estimation in an industrial batch polymerization process," *Journal of Process Control, 19(3), 520–529.*, 2009.

[47] J. Qin, "Inferences for case-control and semiparametric two-sample density ratio models," *Biometrics, Oxford Press*, 1998.

[48] K. Chen and I. Castillo, "Soft sensor model maintenance: A case study in industrial processes," *IEEE TRANSACTIONS ON AUTOMATION SCIENCE AND ENGINEERING*, 2014.

[49] Y. Liu and T. Chen, "Auto-switch gaussian process regression-based probabilistic soft sensors for industrial multigrade processes with transitions," *Industrial Engineering Chemistry Research, 54(18), 5037–5047.*, 2015.

[50] T. Rehrl, J. Hörmann, "Control of three different continuous pharmaceutical manufacturing processes: Use of soft sensors." *International journal of pharmaceutics, 543(1-2), 60–72.*, 2018.

[51] R.-O. T. and A. Singh, "Near infrared spectroscopic calibration models for real time monitoring of powder density," *International journal of pharmaceutics, 512(1), 61–74.*, 2016.

[52] W. M. Markl, D., "Review of real-time release testing of pharmaceutical tablets: State-of-the art, challenges and future perspective," *International Journal of Pharmaceutics, 119353.*, 2020.

[53] A. L. Mundozah, "Assessing particle segregation using near-infrared chemical imaging in twin screw granulation," *International journal of pharmaceutics, 568, 118541.*, 2019.

[54] V. Pereira, "Exploring process configurations and pat tools in solution preparation," *Universidade de Lisboa, Faculdade de Farmácia*, 2020.

[55] J. Vrentas, "Dissolution of rubbery and glassy polymers," *Proc Phys Soc 92(1):9–16.*, 1967.

[56] B. Narasimhan, "Mathematical models describing polymer dissolution: consequences for drug delivery," *Advanced Drug Delivery Review 48(2/3):195–210*, 2001.

[57] S. Edwards, "Statistical mechanics of polymerized material," *Advanced Polymer Science 128:158–207*, 2007.

[58] N. Peppas, "The physics of polymer dissolution: modeling approaches and experimental behavior," *Advanced Polymer Science 128:158–207*, 2007.

[59] V. Ranade, "Convective diffusion from a dissolving polymeric particle," *AIChE J 41(3):666–76*, 2012.

[60] I. Devotta, "The life time of a dissolving polymeric particle," *Chemical Engineering Science 49(5):645–54*, 2014.

# A

# Appendix

## A.1 Polymers and Nomenclature

***CONFIDENTIAL***

## A.2 Methodology-Dissolution Tests

***CONFIDENTIAL***

## A.3 Experimental Dissolution Results

***CONFIDENTIAL***